Metatech

Meta-R-320

The Early-Time (E1) High-Altitude Electromagnetic Pulse (HEMP) and Its Impact on the U.S. Power Grid

Edward Savage
James Gilbert
William Radasky

Metatech Corporation
358 S. Fairview Ave., Suite E
Goleta, CA 93117

January 2010

Prepared for

Oak Ridge National Laboratory
Attn: Dr. Ben McConnell
1 Bethel Valley Road
P.O. Box 2008
Oak Ridge, Tennessee 37831
Subcontract 6400009137

2.6 HOB Variation

Note that the burst is described as being exoatmospheric – above the atmosphere. Except for various effects that can occur on satellites and very long range communications, the nuclear burst may not produce any other effects on man except through its HEMP. There is no exact criterion for HOB (height of burst) that qualifies for HEMP; however HEMP varies with HOB, as shown by the sample results in Figure 2-6. The average result (violet line) is averaged over the full exposed region, which is larger for higher HOB. For each weapon there is an optimum burst height to produce the maximum peak HEMP E field – usually somewhat less than 100 km. As one goes lower in HOB, the peak HEMP E eventually falls, and starts falling significantly when the burst locations gets into the atmosphere – typically we might ignore E1 HEMP when the HOB gets below about 20 km (again, an approximate altitude). Going to altitudes above the peak HOB, the peak HEMP E falls gradually, so that there might be some E1 HEMP when the burst is greater than many multiples of 100 km. Again, the exact details of the HOB variation (and other variations, such as with observer position) depend on the burst (the weapon parameters).

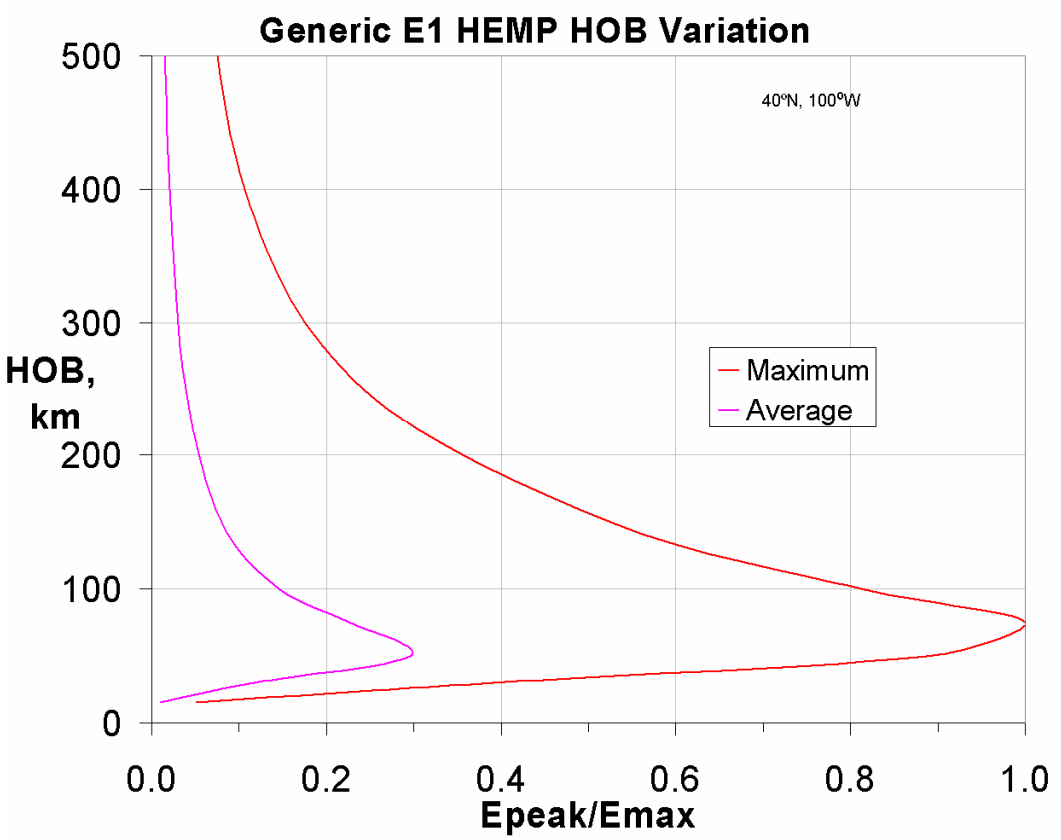

Figure 2-6. Sample E1 HEMP HOB variation. This shows the HOB variation, for a typical device, for the highest E1 peak seen over the full exposed region (red line), and for the average E1 Peak – averaged over all the exposed area. The E1 peak levels are plotted as a fraction of the absolute maximum E1 HEMP for all burst heights (it occurs about HOB=75 km in this case).

2.7 Exposed Region

However, besides the variation of the maximum E peak with HOB, there is also a variation in the area coverage – the amount of the Earth's surface that is exposed to the E1 HEMP. This is simply determined by geometry – a given point on the Earth will be illuminated by E1 HEMP if it is within line-of-sight of the burst location. (For such determinations, for simplicity, the Earth is usually just assumed to be a sphere, ignoring topography and the Earth's slight ellipsoid shape.) Figure 2-7 plots the radius of the exposed region versus burst height, and Figure 2-8 plots the area. Figure 2-9 shows area coverage for a burst over the U.S., for several burst heights.

As can be seen, a very large area is exposed to the E1 HEMP. Going higher (HOB higher) increases the area coverage, however, note that the ground range increase is sub-linear with HOB – the area coverage is approximately linear in burst height. Also, the E1 HEMP strength tends to have its maximum for HOBs below 100 km, and so above that the extra area coverage for higher HOB comes at the expense of lower field levels.

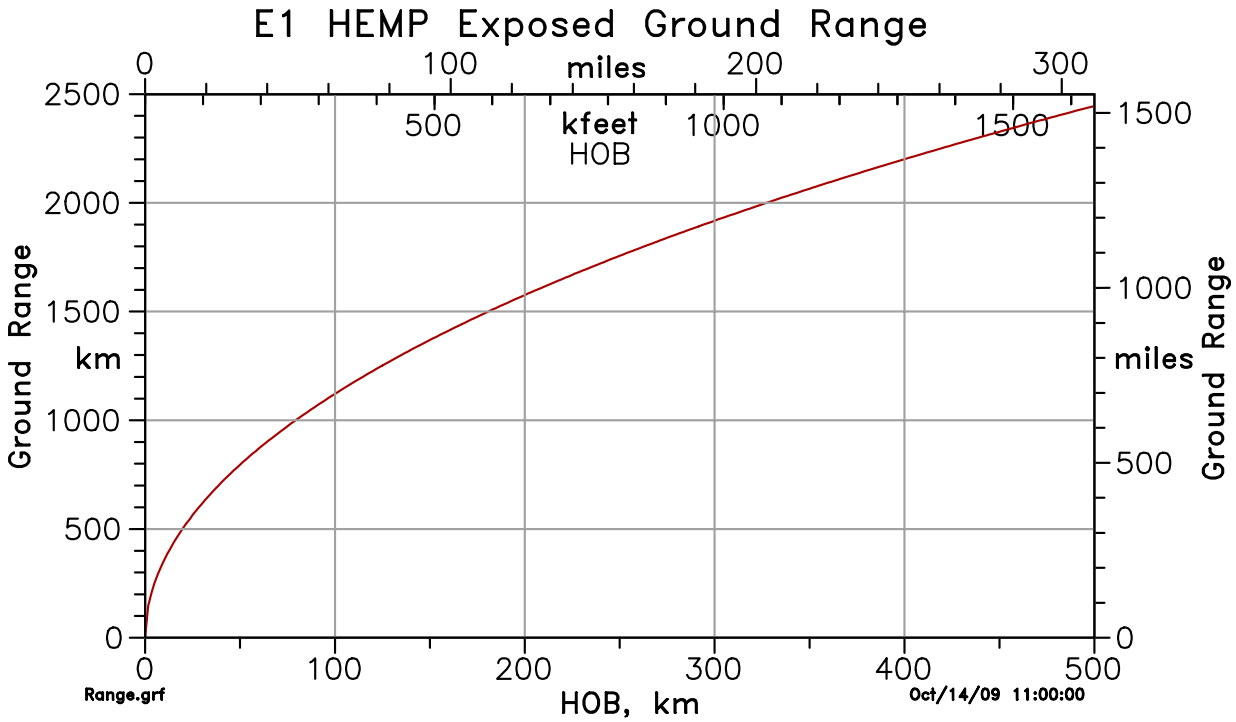

Figure 2-7. Radius of the E1 HEMP exposed region on the Earth versus the burst height.

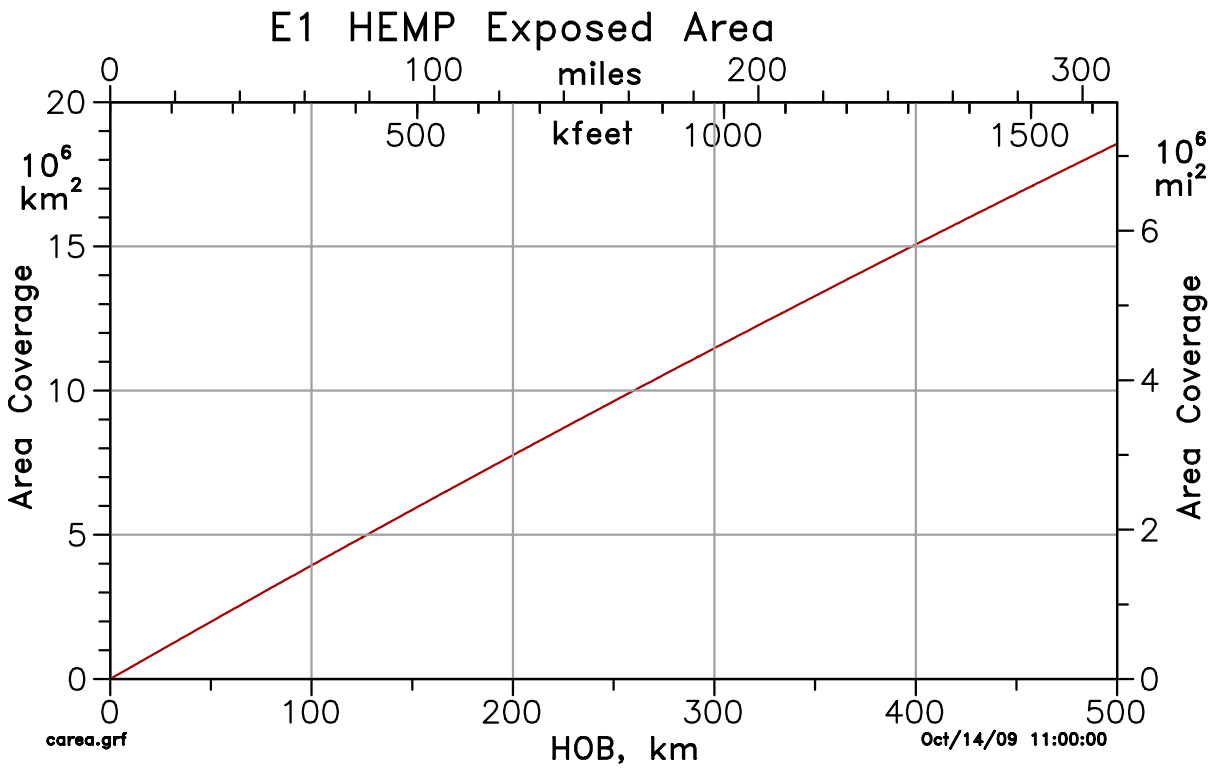

Figure 2-8. E1 HEMP exposed region area versus burst height. The area is given in million of square kilometers (left axis) or square miles (right axis). The continental U.S. has an area of about 8.0 million square kilometers (3.1 million square miles).

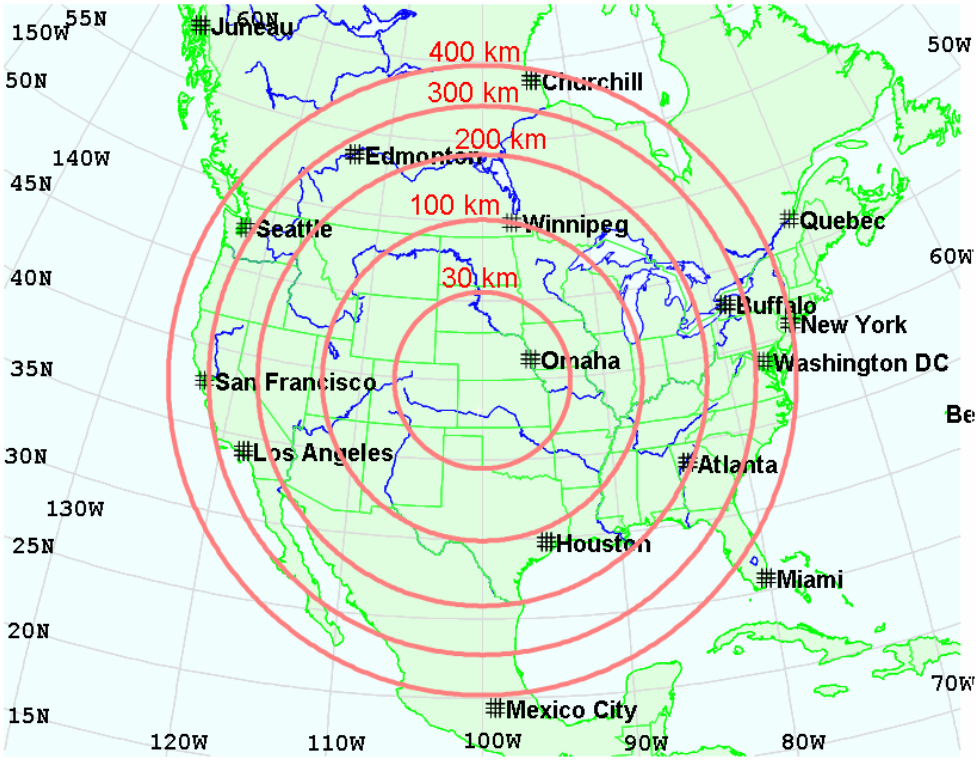

Figure 2-9. Samples of E1 HEMP exposed regions for several heights. The red circles show the exposed regions for the given burst heights, for a nuclear burst over the central U.S.

2.8 E1 HEMP Geometry Features

There are a few common geometric features for a "smile" diagram. Figure 2-10 shows a north-south cut cross-section through a burst point in the northern hemisphere (all results shown in this report are for the northern geomagnetic hemisphere, and many results are shown for a burst over the central U.S.). The view is from the west, looking east, with the north to the left and the south to the right. This figure shows the three special points, and the tangents. The rays originating at the burst and that are tangent to the Earth's surface define the maximum extent of the E1 HEMP exposure region, as discussed in the previous subsection.

Ground Zero (GZ) is the point directly below the burst – the observer ray goes straight down. This is the center of the smile diagram. Also, often observer points are located in terms of "ground range" – this is the distance, along the Earth's surface, from GZ to the observer (a full location determination would then also require the observer's azimuthal angle, such as measured clockwise from the north direction).

The red region in the atmosphere is the "source region" – its boundary depends on how we want to define it, but could be assumed to be, for example, the region between 20 and 40 km in altitude. The GZ ray goes through the source region most directly, and for the tangent point the ray is more oblique, taking a longer path in going through the source region layer. (We can also see that the spherical divergence effect – $1/r^2$ fall off – means the level of the gammas reaching the source region is less as we go out from the GZ point.)

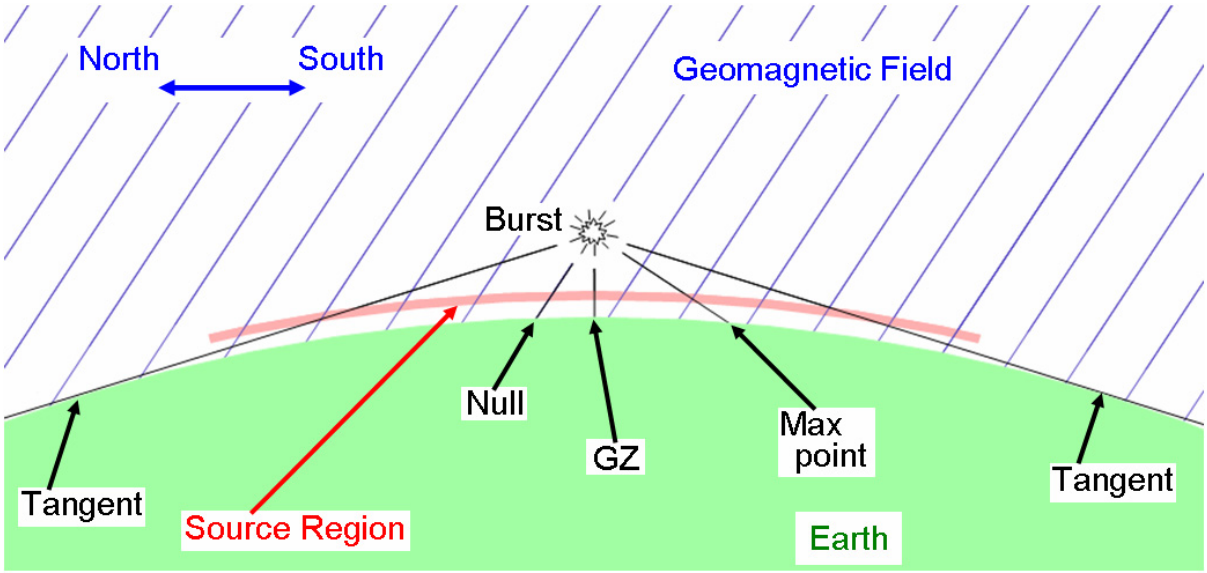

Figure 2-10. Explanation of smile diagram variation along the center north/south line. This is a cut through the center, with north to the left, and south to the right, for a northern hemisphere burst. (For the southern hemisphere the null point is on the south, and the max point to the north.)

The bottom edge of the source region could be defined relative to the "breakaway point". On the ray from the burst to the observer, the level of the gammas decrease along its path through the source region, and the level of the E1 HEMP increases. At some point the gammas are too weak to contribute much more to increasing the level of the E1 HEMP, nor to generated high enough air conductivity to erode away much of the E1 HEMP field. This is essentially the bottom edge of the source region. This is called the breakaway point – for points further down the ray the E1 HEMP is now a free wave, with no more effects from the sources and conductivities of the source region. This is really an arbitrary point, because the gamma effects do not suddenly stop at any point, but decrease smoothly (but sharply) with increasing air density. Often some criterion is used to define breakaway, such as the condition

$$\frac{\sigma}{d\sigma/dz} < \frac{2}{Z_o \sigma} \qquad \left(\text{the right hand side is an approximation to } \frac{E}{dE/dz} \text{ in conductive air} \right)$$

where σ is the air conductivity, E is the electric field (both vary with time), and Z_o is the impedance of free space (about 376.7 ohms). (The right hand side is the attenuation distance of EM waves for $\sigma \ll \omega\varepsilon_o$.) This condition says that the conductivity is falling faster (relatively) with lower altitude than the relative fall in the E field due to conductivity. Generally we would want to take any E1 HEMP calculations to slightly lower altitudes. (Although often a simpler lower altitude criterion is used – assuming the bottom of the source region has been hit when the calculated rE product, E times distance from the burst, did not change significantly from the previous calculational position.)

The other two special positions in Figure 2-10 are related to the geomagnetic field. The "null point" is where the observer ray and geomagnetic field lines are parallel. For this point the E1 HEMP is very low (ideally it would be zero). On the opposite side of GZ is the "max field point" (or "max point" for short). This term has been used to name the location on the smile diagram where the E1 HEMP has its maximum peak level. There are two effects involved in this – one is that the most direct rays through the atmosphere generally produce the highest E1 levels, and so this would favor the GZ ray. However, the second effect is the angle at which the observer ray crosses the geomagnetic field lines – favoring the point at which they are at right angles. This point could be called the "geomagnetic max point". Note that the max field point depends on both the device and geometry, while the geomagnetic max point only depends on geometry.

For the northern hemisphere, generally the max field point is a little north of the geomagnetic max point – pulled away from the point of being at right angle to B_{Geo} by the better angle through the atmosphere nearer to GZ. However, there is a third effect that also sometimes comes into play. This involves the breakaway point. For very large gamma outputs and very lower burst heights, the breakaway altitude may be pushed very low, especially for straight down rays. At such low altitudes the Compton electrons have shorter life times, thus less turning in the geomagnetic field and so less total source current to generate the E1 HEMP. Thus, for such cases (large gamma output, very low HOB), the atmosphere angle variation might not be best straight down – there it might actually be significantly suppressed. In that case the max field point might vary from the

usual position of being a little north of the geomagnetic max point, and actually be south of the geomagnetic max point, especially for lower geomagnetic latitudes.

Note that for this report we will often mean "geomagnetic max point" when we use the "max point" term. The geomagnetic max point depends only on the geometry – the burst location (latitude, longitude, and height) – while the actual maximum field point, typically slightly to the south of GZ for a northern hemisphere burst, also depends on the characteristics of the nuclear explosion, and so varies from weapon to weapon.

Figure 2-11 shows two plots – it gives the ground range from GZ to the null point (on the left) and geomagnetic max point (on the right) versus HOB (burst height), for various geomagnetic latitudes. (For example the position 40°N, 100°W, in the central U.S., has a geomagnetic dip angle of 67.55°, and geomagnetic latitude of about 50.43°N.) Different horizontal axis scalings are used for the two sides of the figure. The solid green line (to the left on both sides of the plot) is for the 10°N geomagnetic latitude positions, and then higher latitudes (closer to the geomagnetic poles) lines are to the right, up to the dashed red line for 80°N. The null point is always near GZ – the farthest it is away is for a burst near the equator. As seen, it is about 700 km away from GZ, out of the maximum E1 radius of about 2400 km, for a 500 km HOB. (The blue line on the right side gives the tangent ground range.) For the geomagnetic max point the variation is the opposite – the maximum range from GZ is for the higher latitudes; and it gets so far out that for the 75°N and 80°N cases the max point gets out to the tangent point and beyond for higher burst heights (the red lines go out to the blue line).

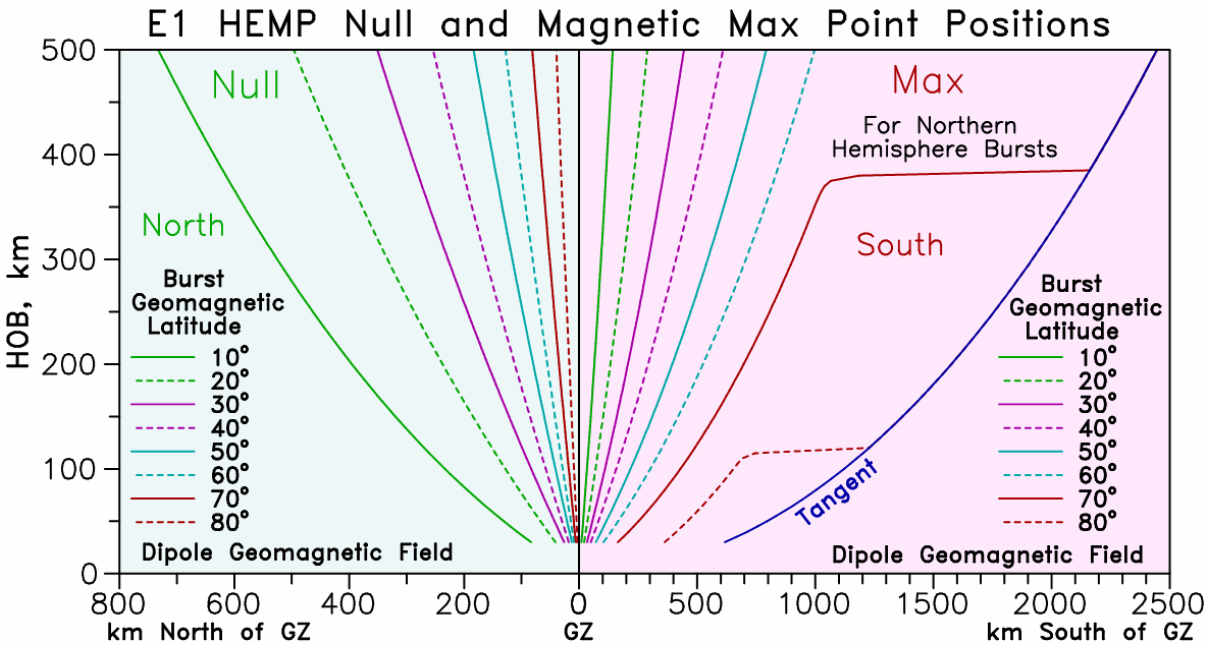

Figure 2-11. Positions of two special E1 HEMP points versus burst height. The position of the null point is on the left side of plot, and the geomagnetic max point is on the right side of plot (different x axis scalings are used in the two sides). This is for an ideal dipole model of the Earth's geomagnetic field. The lines are for 10° increments in geomagnetic latitude (solid green for 10° above the equator, up to dashed red for 80°, which is 10° from the magnetic pole).

Table 2-4 summarizes some characteristics of this generic E1 HEMP signal. By construction, is has a peak of 50 kV/m. The peak power is very high, but the total energy (approximately peak power times pulse width) is modest. The pulse rises in a few nanoseconds, and has a pulse width of about 23 nanoseconds. The spectrum extends well above 100 MHz.

Table 2-4. Characteristics of the IEC E1 HEMP waveform.

IEC E1 HEMP Waveform Properties	
Characteristic	Value
Waveform peak	$E_{peak} = 50{,}000\,V/m$
Spectrum peak	$E_{low\ freq} = 0.00152\,V/m/Hz$
Waveform peak power	$P_{peak} = 6.64\times10^{6}\ W/m^2$
Spectrum peak power	$P_{low\ freq} = 6.11\times10^{-9}\ W/m^2/Hz$
Total energy	$W_{total} = 0.115\,J/m^2$
Time of peak	$t_{peak} = 4.84$ ns
Rise time, 10% to 90% of peak	$t_{10-90} = 2.47$ ns
Pulse width, full width at half maximum	FWHM = 23.0 ns
Pulse width, total energy over peak power	$W_{total}/P_{peak} = 17.3$ ns
Spectrum width, total energy over peak spectrum power	$W_{total}/P_{low\ freq} = 18.8$ MHz

To get a feeling for this E1 HEMP signal, consider another EM signal – a FM radio transmission at 100 MHz. Assume the transmitted power is 10,000 watts (RMS), and we are receiving the signal close by, at a distance of 1 mile (1.61 km). For a crude estimate, assume a transmitting antenna gain of $\sqrt{2}$ (2 in power). Then the peak power at the 1 mile range is 1.23 mW/m^2, and the peak electric field is 0.68 V/m. Thus, this signal is smaller than the E1 HEMP electric field peak by a factor of 73,500 – or a factor of 5.4×10^9 in power (97.3 dB). Figure 2-14 shows the IEC E1 HEMP waveform, compared to the FM radio signal – scaled up to the same amplitude. We can also see that the rise of the E1 pulse is similar to the rise of a cycle of the FM signal, and so we can see that the E1 HEMP does have signal content up to 100 MHz. Figure 2-15 shows the actual spectrum of the E1 HEMP waveform.

Certainly the E1 HEMP signal is much larger than the FM radio signal. However, the E1 HEMP energy density is modest - 0.114 Joules/m^2. By contrast, about every 3.1 minutes the FM radio signal delivers the same amount of energy density (of course the E1 HEMP delivers its energy in a few tens of nanoseconds, and over a much larger area). This is an energy density – the amount of energy going by through an area of a square meter. In general it would also be about the amount of energy picked up by a wire antenna about a meter long. Coupling collection areas can vary quite a bit, of course. For example, a long wire could collect significantly more than 0.114 Joules.

Now that we have the amount of weapon energy that can generate E1 HEMP, we will consider the total energy in the E1 HEMP. We will use the IEC E1 HEMP signal defined previously, which had a peak of 50,000 kV/m at the strongest point on the Earth, and energy density of 0.115 J/m^2. The exposed region goes out to the tangent of 972.8 km, an area of

$$A_{E1} = \pi(972.8\text{ km})^2 = 2.973\times10^{12}\text{ m}^2$$

(more accurately, accounting for the Earth's curvature, it is actually 2.967x10^{12} m^2). The 50,000 kV/m is the E1 HEMP at the maximum point; it is less elsewhere, as previously shown in Figure 2-3. Averaged over the exposed region, for this case the peak is 0.1243 of the maximum (so about 6.21 kV/m). Thus, the total energy in the E1 HEMP is

$$W_{E1} = 2.967\times10^{12}\text{ m}^2 \times 0.1145\text{ J/m}^2 \times 0.1243^2 = 5.25\times10^9\text{ J}$$
$$= 1457\text{ kW} - \text{hr}$$

(approximately 53 days of electricity for a typical U.S. household). This E1 HEMP energy is only about

$$\frac{W_{E1}}{W_\gamma} = \frac{5.25\times10^9\text{ J}}{8.87\times10^{11}\text{ J}} = 0.59\%$$

of the energy in the gammas that generate the E1 HEMP. This is also only

$$\frac{W_{E1}}{W_{500kT}} = \frac{5.25\times10^9\text{ J}}{2.09\times10^{15}\text{ J}} = 0.0000025 \quad \text{(fraction, not percent)}$$

of all the energy from the burst. Thus, the E1 HEMP total energy is only a small fraction of the energy of the burst output gammas that go into generating it. The rest of the gamma energy goes into losses, such as what ultimately ends up as heating the source region, or radiating energy away from the source region (as photons: gammas, x rays, ultraviolet, infrared, etc.). Part of the lost energy was initially converted to EM energy, but ended up being lost to heat due to the air conductivity. Again, we need to emphasize that the E1 HEMP may have a small fraction of the burst's output, but it is a coherent, high level, EM pulse that is delivered very quickly. The total peak power from of the E1 HEMP is about

$$\frac{5.25\times10^9\text{ J}}{17.25\text{ ns}} = 3.0\times10^{17}\text{ watts}.$$

Again, we note, this is an extremely high level partially due to the very short time duration of the pulse.

2.12 E1 HEMP: Instantaneous and Simultaneous

E1 HEMP has been described as instantaneously and simultaneously blanketing a continent size region. How fast is this really? We have seen that the E1 HEMP pulse is very fast – for example, the IEC waveform is 23 nanoseconds wide. And it also hits the entire exposed region essentially at once. This is because the speed of light applies – to the gammas and to the E1 HEMP signals. For a 100 km burst (62.1 miles), various time delays are:

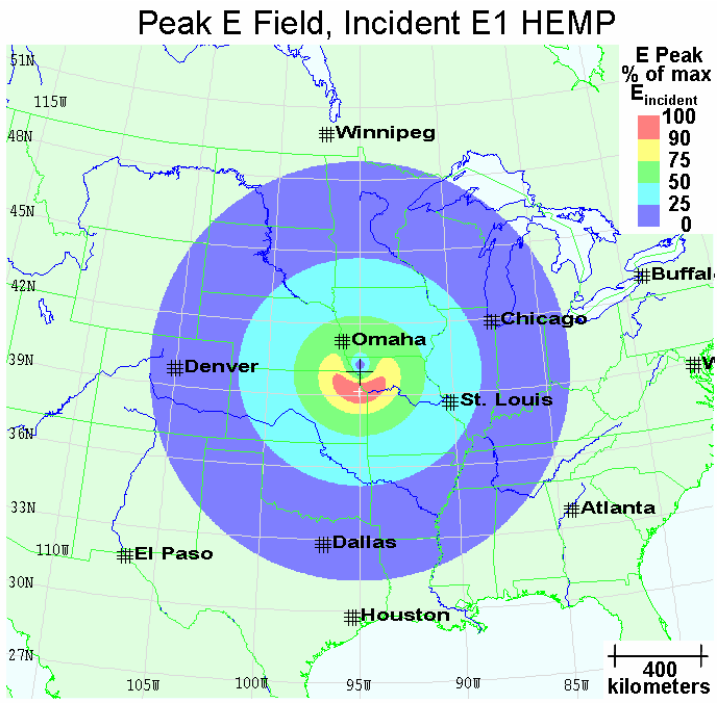

Figure 2-17. Sample E1 HEMP peak contours. This plots the peak value of the incident E field total waveform. The burst height is 75 km. The contours are as percentages of the absolute highest peak, which occurs at the point marked by the white cross hairs, south of the burst position (GZ, marked by the black cross hairs).

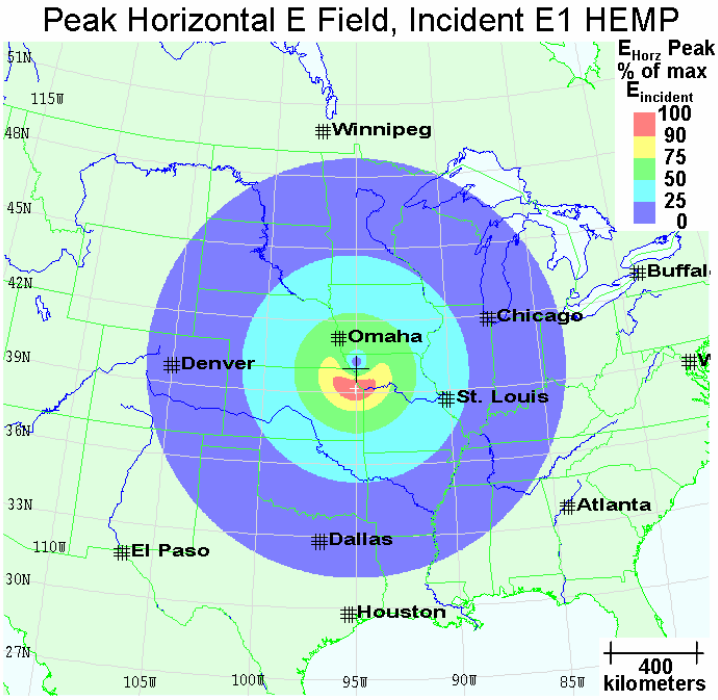

Figure 2-18. Sample E horizontal component contours. For the sample case of Figure 2-17, this gives a contour plot of the peak of the horizontal component of the incident E1 HEMP E field. The contour edges are at the same field level values as for Figure 2-17 (both use the same percents of the maximum peak magnitude of the incident field).

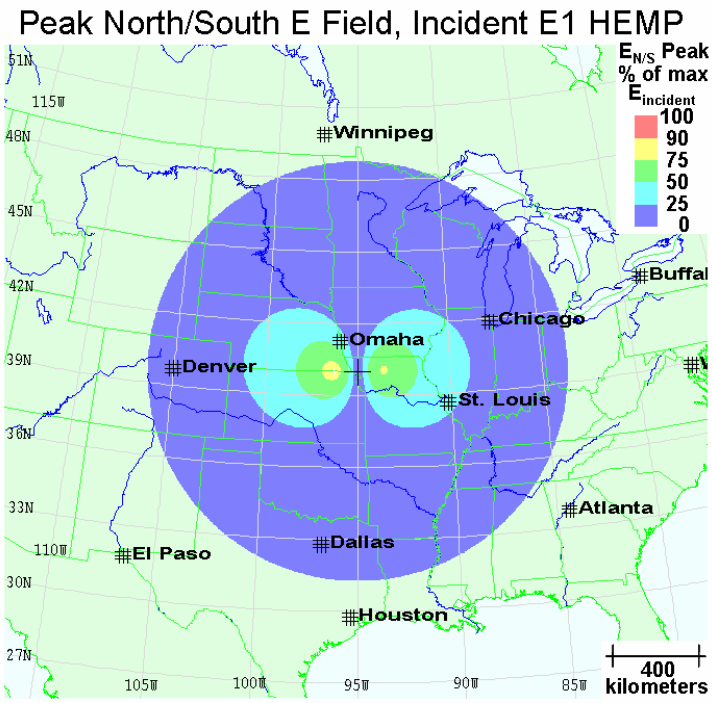

Figure 2-19. Sample E north/south horizontal component contours. This and the next figure break down the horizontal term (Figure 2-18) into two components. These contours show the North/South component of the peak E1 HEMP incident E field. (Again this uses the same E field values for edges of the contour set.)

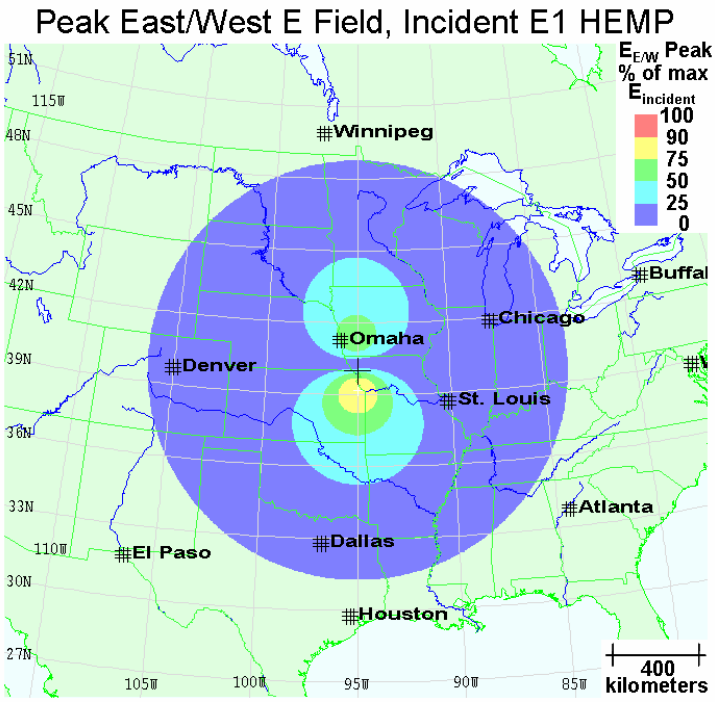

Figure 2-20. Sample E east/west horizontal component contours. This shows the other horizontal component for the E1 HEMP sample – the East/West part of the peak E field (using the same contour set values as the previous plots).

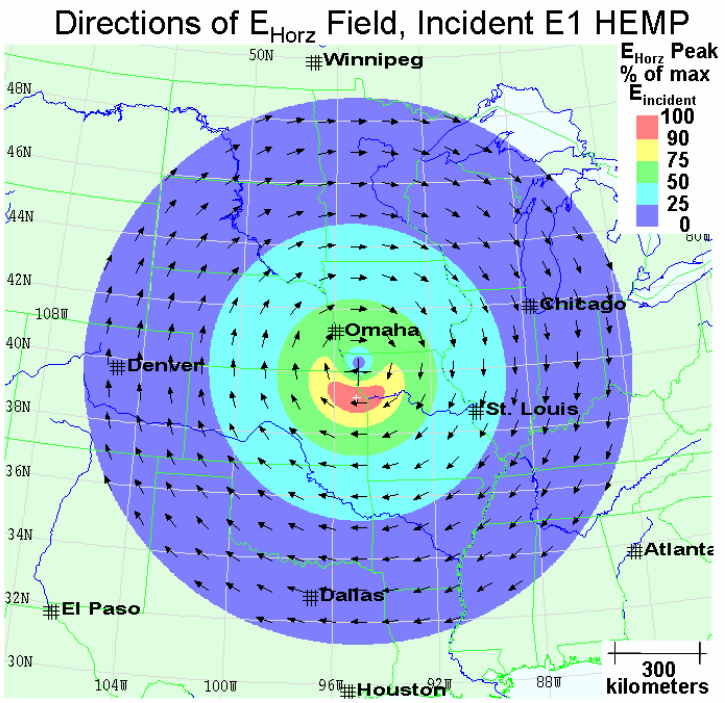

Figure 2-21. Horizontal E field direction for E1 HEMP sample. Arrows show the E field directions for the horizontal E field peak for the sample case. The contours are for the peak horizontal E field – the same as in Figure 2-18. (Here we have zoomed in a little more than for the other figures.)

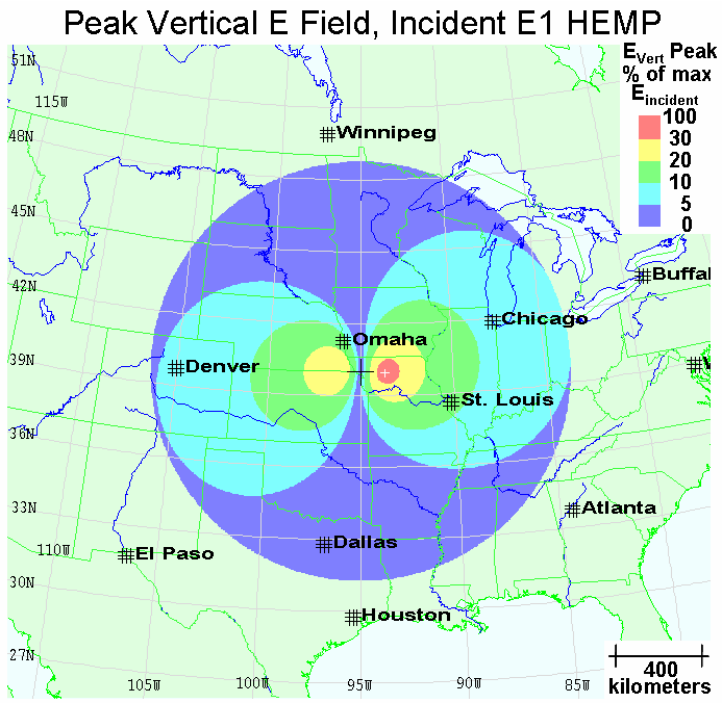

Figure 2-22. Sample E vertical component contours. This gives the peaks of the vertical component for the E1 HEMP sample. Here a different contour levels set is used, since the vertical values tend to be somewhat smaller than the horizontal values (but the contours still use percent of the maximum total incident E field value).

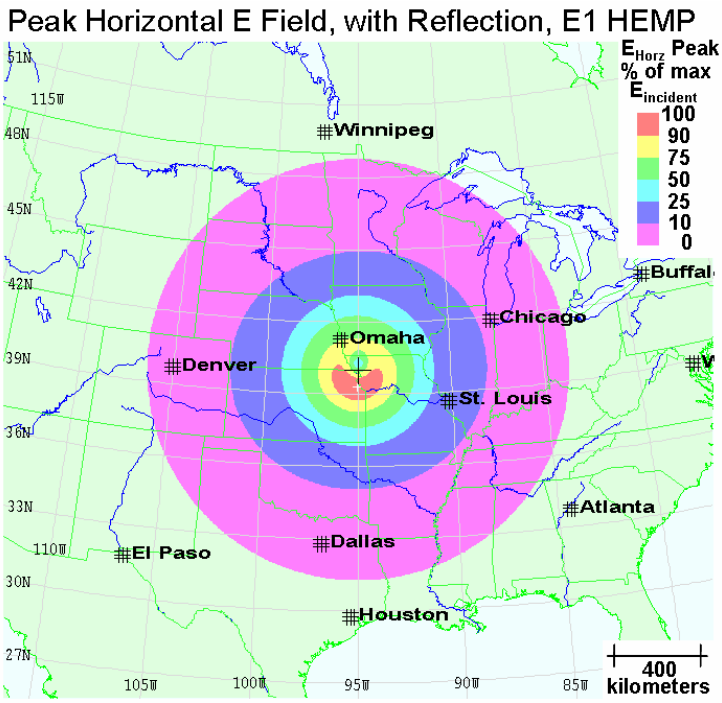

Figure 2-23. Peak horizontal E1 HEMP contours, including ground reflection. We have added a 10% contour level for this plot. (Parameters: 10^{-2} S/m ground conductivity, observer 3 meters off ground.)

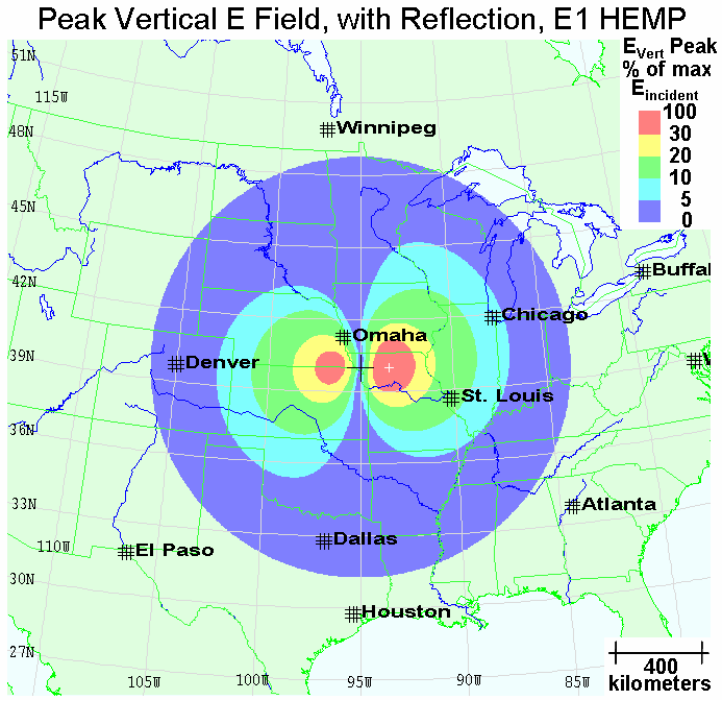

Figure 2-24. Peak vertical E1 HEMP contours, including ground reflection. (Parameters: 10^{-2} S/m ground conductivity, observer 3 meters off ground.)

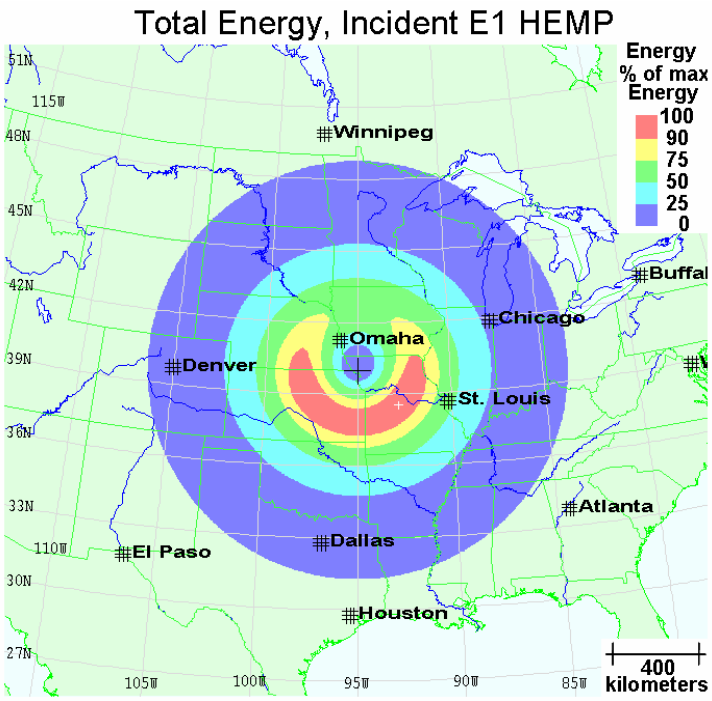

Figure 2-25. Sample E1 HEMP total energy contours. This plot shows the total electromagnetic energy in the incident E1 HEMP. The contour set uses percents of the value at the peak point.

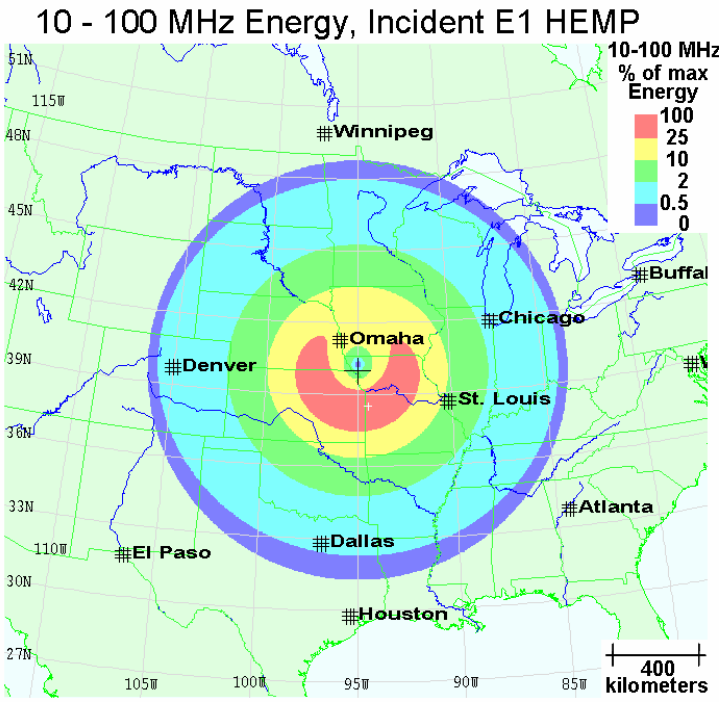

Figure 2-26. Contours of energy in the 10 to 100 MHz band. This is like the previous plot, but for only the energy in 10-100 MHz. The contour values are as percentages of the value of total energy at the maximum E1 HEMP energy point (the same normalization used for Figure 2-25).

2.14 E1 HEMP Effects on Systems

E1 HEMP peak field levels can be very high, and certainly there could be some devices within a system that have some vulnerability to such high levels. However, typically vulnerabilities involve the intermediate step of having voltages and currents generated on a conductor, and then that signal getting to the fragile device. The conductor might be deep within the system, such as wiring in the internal circuits, however a major concern is external cabling attached to the system, for two reasons. First, outside wiring can be very long, which tends to increase coupled signal levels, while internal wires are limited by the enclosure size. Secondly, the system enclosure and support structure, especially if metallic, attenuates electromagnetic fields and leads to lower coupling for internal wires.

With a peak field of 50 kV/m, even a short "antenna" 10 cm (4 inches) long can mean a voltage of about 5000 volts, and it could be much higher for longer lines. Power lines, of course, can be very long. Other possible long lines include communication lines within a facility, such as network lines and phone lines. For power substations there are also the various sensing and activation lines used for the relaying process that maintains power reliability and tries to lessen harm to the power system from faults.

With the advance of modern systems, and miniaturization of components, the normal operating voltages of systems tends to be a few volts, and so HEMP levels of thousands of volts or more cannot be good for the system. Also, the operating frequencies of systems, such as computers and various types of controllers, are such that an E1 HEMP pulse would cover many clock cycles. Thus the fact that E1 HEMP type pulses can have effects, as has been found in vulnerability tests, is not surprising.

Typically system effects are separated into two types (although finer gradation is possible):

Temporary Upset
Permanent Damage

Damage is fairly clear – something physically happens to some part of the system, such that the system no longer works. Sometimes the damage might be readily seen, such as a device "blown up", but other times there may not be any visual damage, yet the system will not work. It might be that the damage is to a small, but critical, area inside an integrated circuit (IC). With devices being microscopic, it is believable that even very small energies could be worrisome. This is why ESD (electrostatic discharge) is such a concern when handing modern electronics. Besides outright damage to a device, we can also have degradation, in which the device still operates, but its performance is not as good as before the assault by the high level pulse. Damage can also be ranked by how long it would take to repair, or how easily it could be fixed. In many cases it would involve determining that there is a problem, and what subsystem is broken, and replacing the subsystem. It might not always be obvious that there is a problem, such as for functions that are only used occasionally. For example, damage to some part of the fault protection for a power substation might not be detected until a fault happens, and the protection does not work properly. In some cases, damage that completely brings down a system might be better than subtle, less obvious, damage. It might be better to know

there is a problem, and so try to fix it, than to depend on some function working properly when needed, only to have that function fail at the critical time.

For EMP vulnerability, it can be very important whether the system is powered up or not. Certainly a HEMP coupled pulse could cause damage, whether it produces no easily seen evidence of the damage, or blows a device apart, as shown in Figure 2-27. Typically the pulse amplitude level needed to cause damage is higher for narrow pulses than wide pulses, and the susceptibility levels for E1 HEMP are higher than for some other types of effects. However, E1 HEMP coupled levels can get very high, and the coupling to long cables can produce pulses that are longer than the incident EM pulse itself. So even an un-powered system, attached to long cables, can be vulnerable.

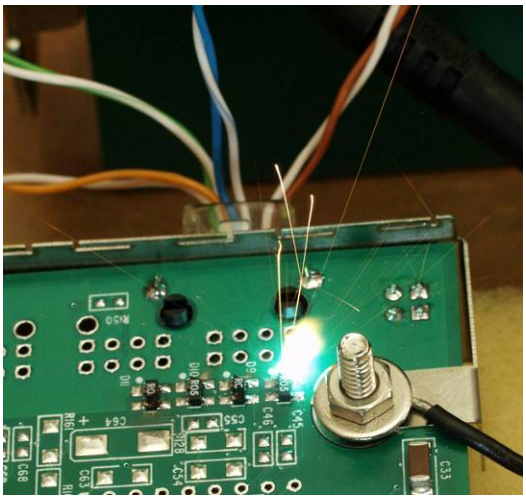

Figure 2-27. Flash and sparks from pulse damage testing. In this case the device under test (DUT) is not powered (not turned on) – the flash in only from the pulser's energy.

However, when a system is powered – actually in an operating state, there can be other vulnerabilities. Even if the incident pulse is low in energy, the system itself typically has access to the power source that runs the system, such as the AC power or a battery supply. The full system gets illuminated by E1 HEMP, so with all the many wires connected to a device are simultaneously assaulted by huge signal pulses, it is very likely the complex circuitry may respond in some abnormal ways. Are any of those responses such that, for example, a high-current arcing path gets created across the power supply – so this short circuit burns out some device along that path? Such effects are very hard to predict, and high-level laboratory tests should always be used if it is important to detect such vulnerabilities.

A classic example of this is found in the TREE discipline (transient radiation effects on electronics). Complementary designs are very common for digital circuits – two transistors are connected in series across the power supply, and the circuit design is such that only one transistor is on at a time. The output level is either high or low, depending on which transistor is on. There can be high efficiency, and little wasteful energy going into heating the wafer in this design, since current might only flow through the series of transistors during switching transients. However, a gamma or x-ray pulse hitting the

active region of the "off" transistor could switch the junction on, just as light does for a photodiode. Once on, there is then a short through the two transistors, and, being microscopic transistors on an IC, extremely little of the energy from the power supply would be needed to heat up and destroy something along the path, such as one of the transistors.

Upset is considered a disruption of the normal operation of the system. It can occur at various levels. There might be a minor glitch, from which the system quickly recovers and continues working. Or it might bring the system down, requiring a "re-boot". The effect might be immediate, or show up later. Some data could be corrupted for a control system, thus leading to improper processing steps, and ultimately some type of failure. For unmanned facilities this might take some time, and again it might not always be immediately obvious that the system is not working correctly, thus leaving the system in a crippled state. That upset could happen is completely understandable. A modern system can be very complex, with many digital signals going around – pulses of a few volts, with switching at frequencies in the megahertz range. When E1 HEMP pulses come in on all of the wires, with much higher voltage levels, lasting for many clock cycles, and with content up to high frequencies, the system could easily get confused.

Under the wrong circumstances, the confusion of an upset could lead to damage, such as if incompatible commands get issued. Such vulnerabilities are often unforeseen. Luckily the world has not experienced real E1 HEMP events that might trigger such unusual, but possibly catastrophic events, but they do occur occasionally due to "EMI/EMC" issues, such as high radar pulses causing a missile on a fighter aircraft to think it has been commanded to fire, while the fighter is on an aircraft carrier deck. Of course, careful design, and extensive testing, can help minimize such possibilities.

2.15 E1 HEMP Coupling

Electromagnetic signals, such as E1 HEMP, generate voltages and currents on conductors exposed to the fields. E1 HEMP coupling is like any other electromagnetic coupling. The EM fields encounter a conductor, and induce voltage and current signals on that conductor. Vulnerability issues occur when the conductor connects to a circuit with parts that could be destroyed or upset.

Coupling is a full electromagnetic effect, but often can be thought of in terms of individual electric (capacitive – see Figure 2-28) or magnetic (inductive – see Figure 2-29) coupling. In these figures we have a cable connected to a metal plate at both ends, such as the shields of a shielded cable that is fully bonded to the metal enclosures where it connects. The same effect applies if the cable is unshielded, except the currents and voltages signals would be seen directly by whatever circuits are attached to the cable ends (with the circuit impedances governing the exact currents and voltages). For capacitive coupling the electric field rearranges electric charges on the conductor – those charge movements are currents, and the force that moves them is a voltage. Similarly, for magnetic coupling, there is an EMF (voltage) generated in the conductive loop by the

time-rate-of-change of the total magnetic flux through the loop, and a current is driven in response.

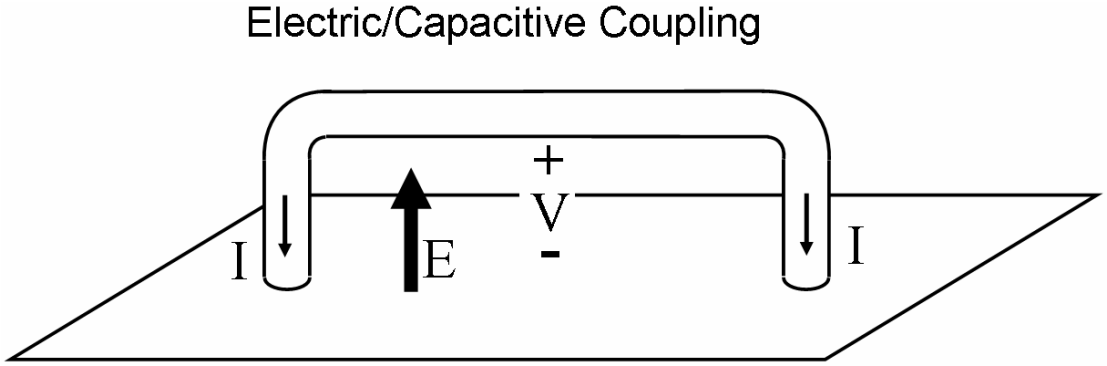

Figure 2-28. Capacitive (electric) coupling to a short cable. The electric field (E) induces the voltages and currents shown.

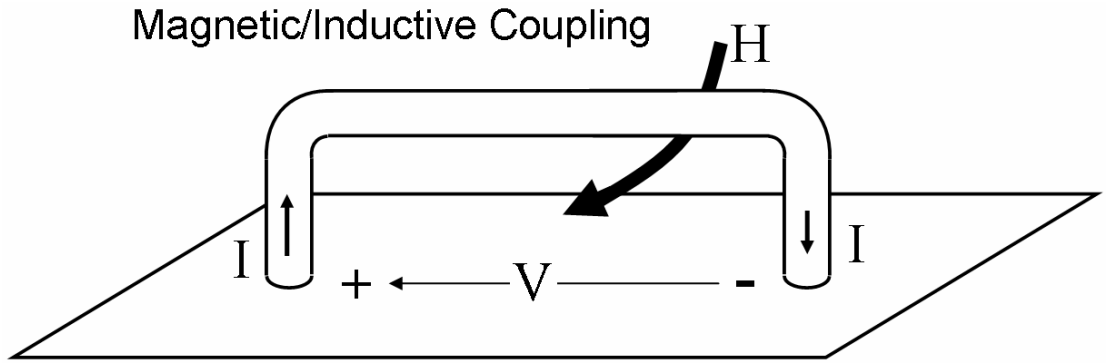

Figure 2-29. Inductance (magnetic) coupling to a short cable. The magnetic field (H) induces the voltages and currents shown.

There are also couplings that are electromagnetic in nature, such as high frequency wave coupling to long cables or antennas. This is exactly the process by which receiving antennas work – and so they will pick up E1 HEMP energy by their very nature. But any conductive object, not just antennas, would have induced signals. The process for antennas and long lines can be very complex, depending on details of exactly which way the incident EM wave is propagating, and the field polarization (which direction the E and H fields point). The E and H must be in the plane perpendicular to the propagation direction, and H must be perpendicular to E in that plane, but otherwise there is no restriction on where E points within the plane (this is the polarization of the field).

Because they can be long, and fully unshielded out in the exposed region, long cabling (lines) are important for E1 HEMP. This applies to lines such as power lines, communication lines, and control lines. In the next three diagrams we continue the pervious set of results – here we show contours of peak currents on wires exposed to the same E1 HEMP as used before. Figure 2-30 shows the peak current on a 100-meter long wire, 5 meters above the ground. This result is for a north/south alignment of the wire, and Figure 2-31 is for an east/west alignment. In Figure 2-32 a vertical wire is used (5 meters long). Current levels get up to hundreds of amps for these coupling examples.

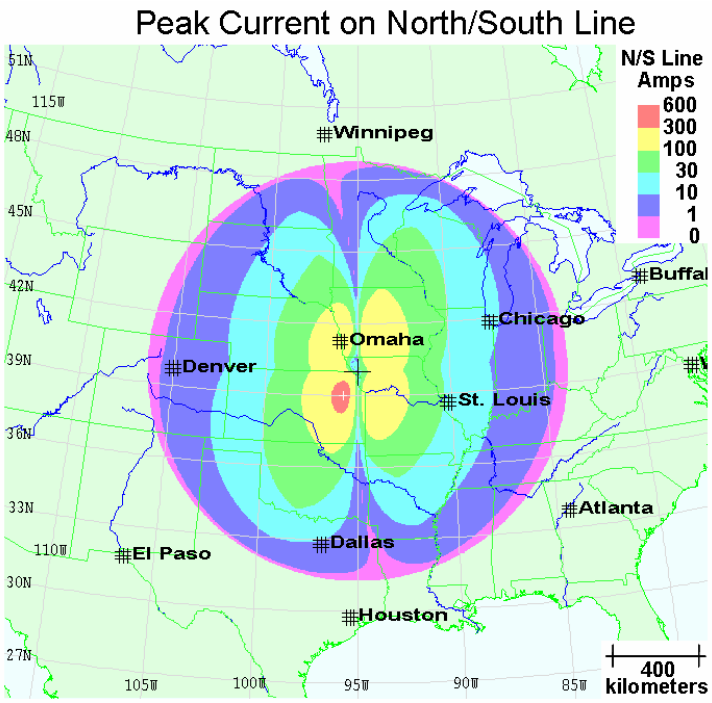

Figure 2-30. Sample contour plot of the peak current on a north/south line. This is for an overhead wire, running north and south, for the same sample E1 HEMP case as the previous contour plots. The line is moved to each observer position to get the data for the contour plot. (Parameters: 10^{-3} S/m ground conductivity, line 5 meters off ground, line 100 meters long, wire 0.2 centimeters in radius.)

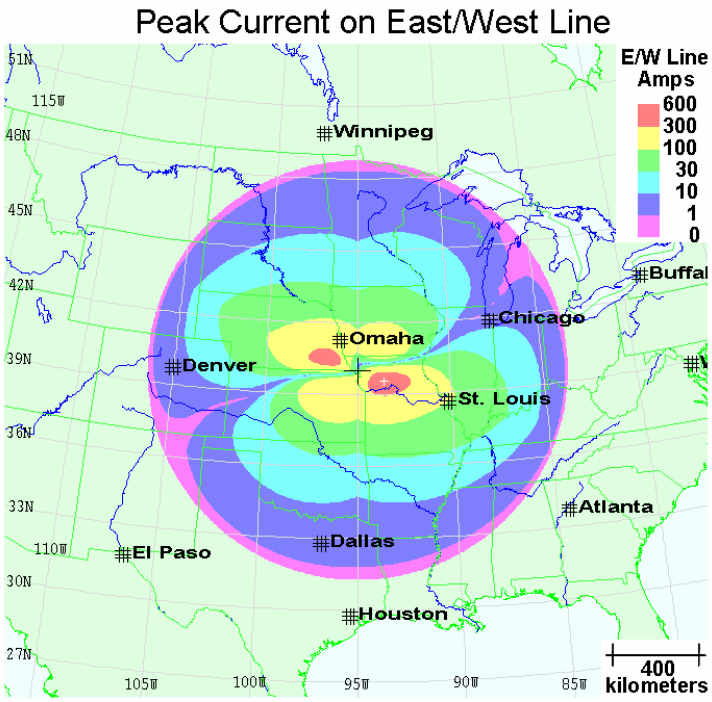

Figure 2-31. Sample contour plot of the peak current on an east/west line. This is the same as in the previous figure, but with the line going east and west. (Parameters: 10^{-3} S/m ground conductivity, line 5 meters off ground, line 100 meters long, wire 0.2 centimeters in radius.)

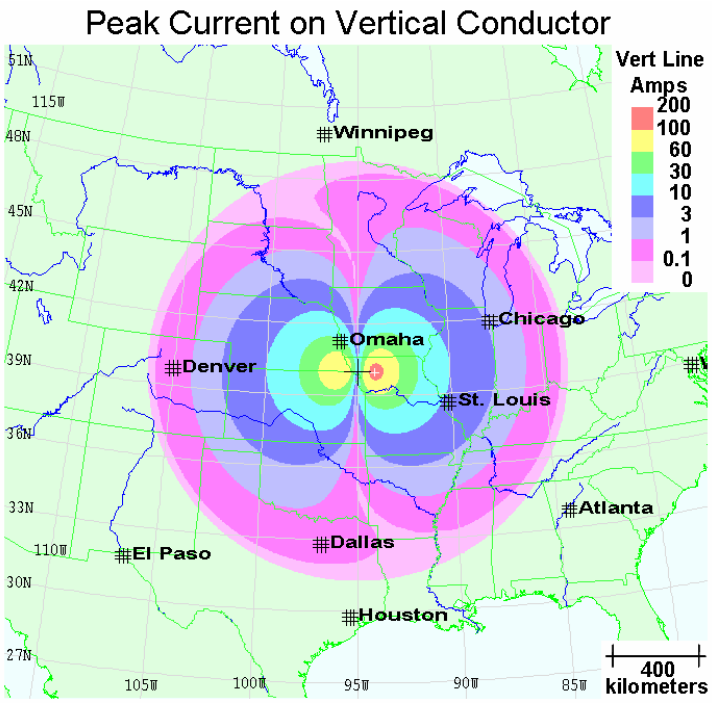

Figure 2-32. Sample contour plot of the peak current on a vertical wire. This is the same case as the previous contour samples, but with a short vertical wire. (Parameters: 10^{-3} S/m ground conductivity, wire 5 meters long, with base on ground, wire 0.2 centimeters in radius.)

2.16 E1 HEMP Penetration and Protection

Typically system vulnerabilities are due to small parts deep within the system, while the assaulting EM environment, such as E1 HEMP, is outside. There are various ways that the external energy can find its way down to the internal devices.

Often (but not always) there is some type of conductive (usually metallic) enclosure around the system. This can provide a barrier to external electromagnetic signals. In fact, a full conductive enclosure is a "Faraday cage", which shields out EM signals by "shorting out" the electric field and reflecting it. A conductive barrier is also associated with the concept of skin depth, introduced earlier:

$$\delta = \sqrt{\frac{1}{\pi \sigma f \mu}} \quad .$$

This gives an indication of penetration depth for EM signals. Higher conductivities (σ) and frequencies (f) mean better shielding. For good shielding, the enclosure thickness should be large compared to the skin depth. Besides being sure the metal is thick enough, we also need to worry about other issues, such as in the following discussions. Generally they are more of a concern than enclosure wall thickness.

The conductive case needs to totally enclose the system to be a good "Faraday cage" – any breaks ("apertures") will allow EM energy to leak in. Figure 2-33 indicates how an external electric field normally "terminates" on a conductor (with surface charge

re-arranging itself on the exterior accordingly). However, if there is an aperture, some of the lines go inside, and end on the interior walls. Thus, some of the EM signal has penetrated inside, and besides the E field, there are the associated magnetic fields, and currents from the moving surface currents. Figure 2-34 shows that magnetic fields parallel to the wall can also penetrate in through the hole and get inside the shield. Surface currents are associated with such magnetic fields, and some of the external current can flow into (and then back out of) the aperture.

Even small holes can be problems for sensitive systems. If made of separate metal plates, the plate seams might have microscopic leaks if pressed or bolted together, and the best approach is for welded seams (and even those need to be tested for leaks after welding, if very good shields are desired). Seams are especially of concern if parallel to the external magnetic field. Such magnetic field orientation implies an outside surface current perpendicular to the seam – and that surface current faces a barrier to its flow when it gets to the seam crack. In diverting that current, some current gets inside the enclosure wall (as shown in Figure 2-34).

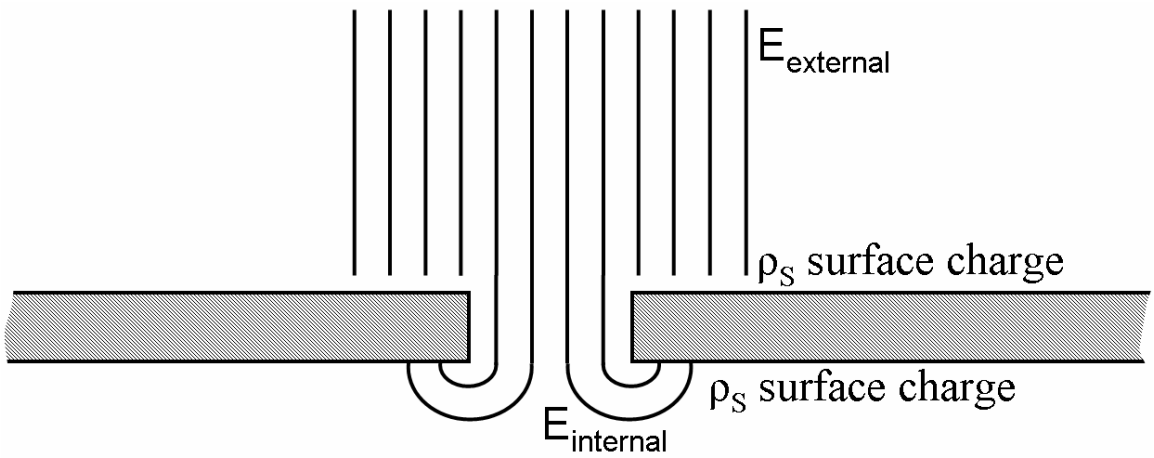

Figure 2-33. Electric leakage through an aperture.

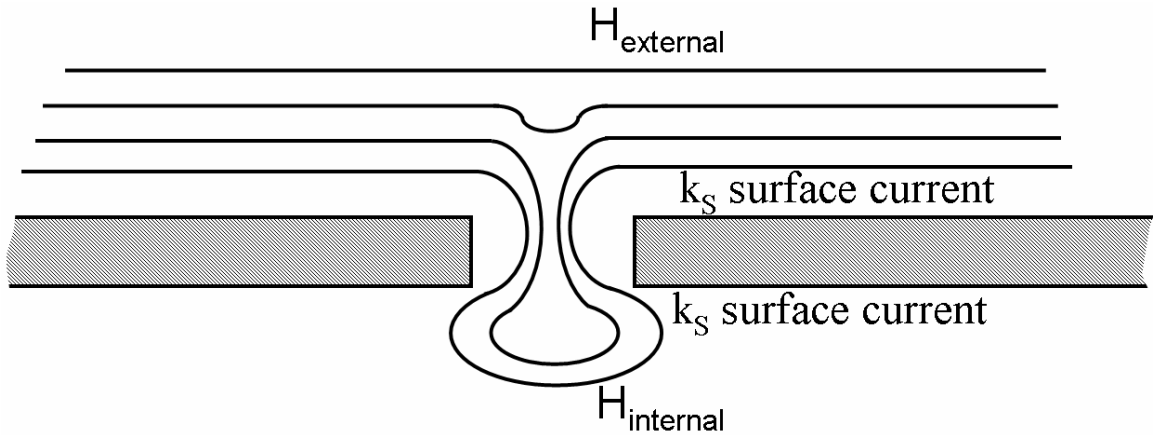

Figure 2-34. Magnetic leakage through an aperture.

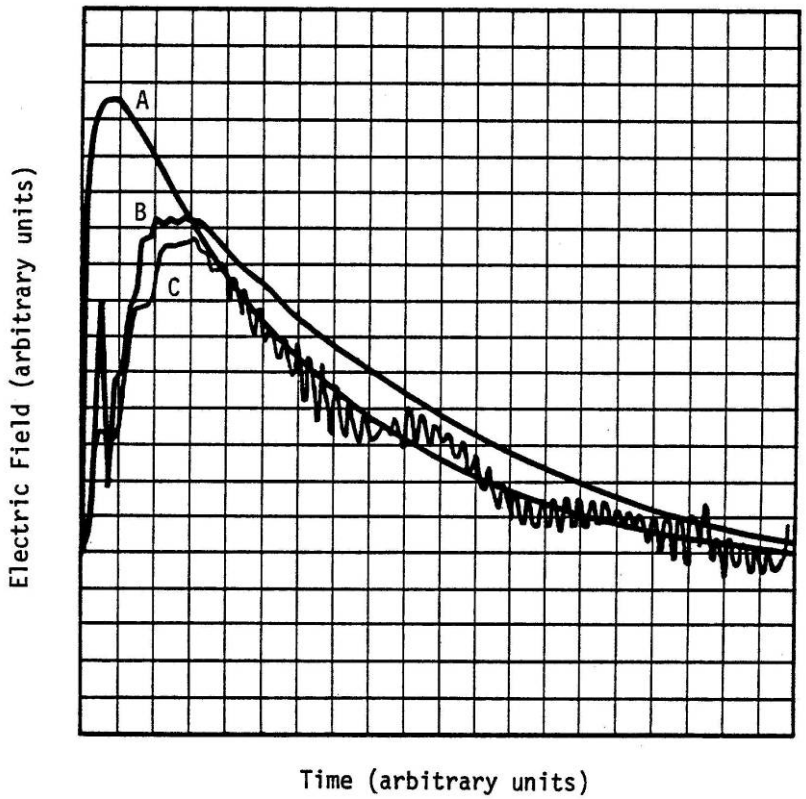

Figure 3-1. Comparison of measured and calculated E1 HEMP signal. "A" is the calculated incident field, and in "B" the effects of the measurement system's distortions are included. These distortions are from the measurement equipment and the antenna (including the metal structure on which the antenna was mounted). "C" is the actual measured E1 HEMP response. (From Daniel F. Higgins and Conrad L. Longmire, "Input to the EMP Interaction Handbook", MRC-R-345, September 1977.)

In the mid 1960s the complete theory (as now accepted) of E1 HEMP was developed, independently by William Karzas and Richard Latter, and Conrad Longmire. After that the theory was refined, and efforts were put into hardening and testing. Numerical codes were developed to calculate HEMP, and numerical fits were found for various parameters involved in the generation process. Generally, the early computer models were constrained by the existing computer resources, and were run on the "supercomputers" of the time. Analytic and numerical models were also developed, and extensively used, to account for EMP coupling to systems.

Much effort was also put into the final step of the HEMP process for system interactions: determining whether a system is disrupted (upset) or damaged by a given HEMP. However, such a system vulnerability evaluation is extremely difficult to do, and attempts at predicting vulnerability levels, and determining in advance where within the system the damage would occur, were typically very inaccurate. Generally tests must be performed instead. Thus, many HEMP simulators were constructed, and test procedures developed. For large size systems, such simulators were large and expensive, and in recent years many have been mothballed.

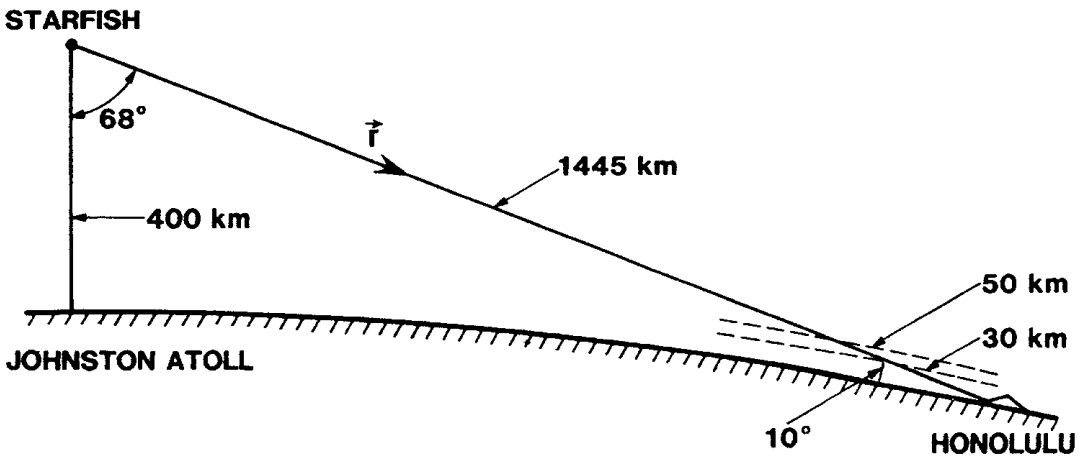

BURST 30 km SW of J.A.
AT 16° 28' N, 169° 38' W

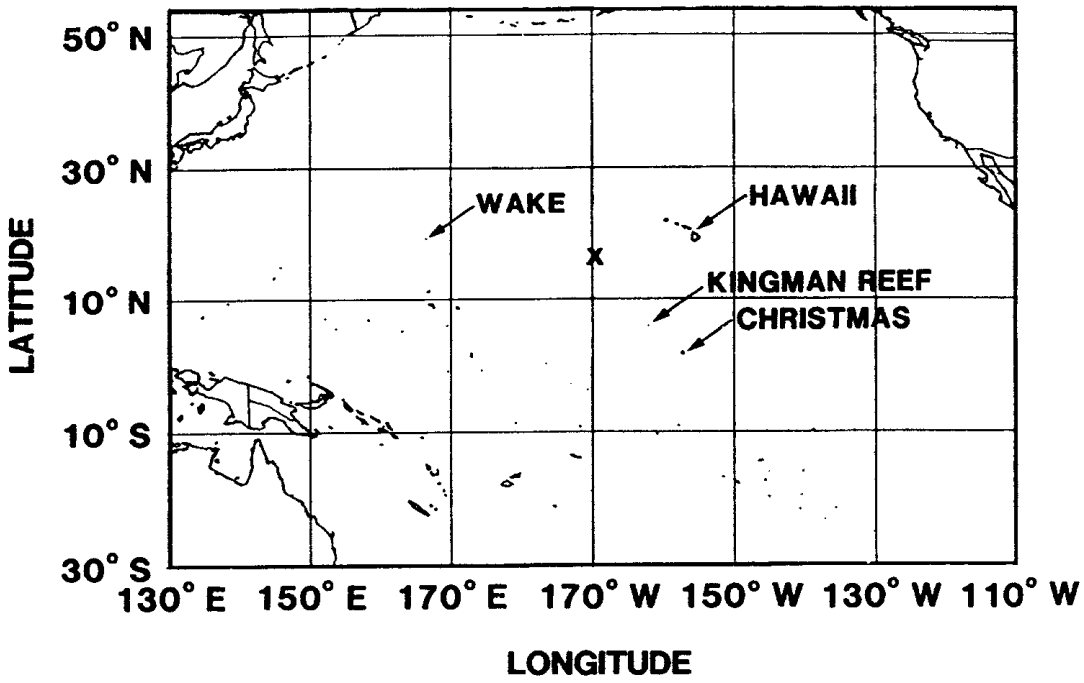

HONOLULU 21.3° N, 157.6° W

JOHNSTON ATOLL 16.6° N, 169.3° W x

Figure 3-2. Geometry of the Starfish test. The "x" shows the burst location. (From: Vittitoe, C., "Did High-Altitude EMP Cause the Hawaiian Streetlight Incident?" Sandia National Laboratories, SAND88-3341, April 1989.)

Electrons moving in a magnetic field (the geomagnetic field in this case) are turned coherently to curve away from their initial forward path, as shown in Figure 4-2. This is the important effect for E1 HEMP – the turned part of the electron's path generates a radiated EM field (just like the electric current driven by the transmitter on an AM station's broadcast antenna). This radiated EM field travels outward, away from the burst point – the same direction as the gammas that are traveling outward. And they both are electromagnetic radiation, and so they both travel outward at the speed of light.

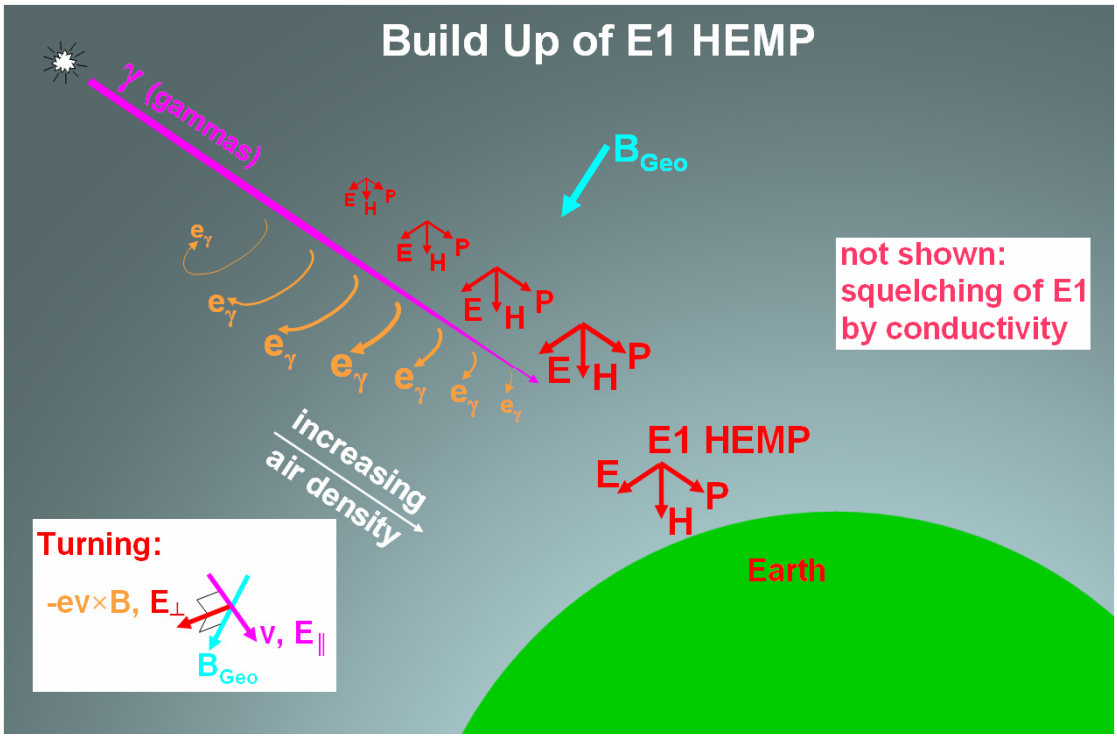

Figure 4-2. Detailed representation of the E1 HEMP generation process. Gammas speed down unaffected in the vacuum of space, until they are low enough to start scattering in the upper atmosphere. Eventually the gamma beam gradually disappears as it transverses more and more air, especially with the increase in air density with lower altitude. Along with scattering that erodes away the gammas, Compton electrons are generated, which turn in the geomagnetic field. The turned path, on average, is longer in thinner air, so there may be more of the spiral path in the higher altitudes than in the lower altitudes. The turned part of the Compton current generates a radiated EM pulse, and this builds up in strength along the burst-observer path (as the gamma beam decreases in its strength). At some altitude the gamma beam is essentially gone, the EM pulse no longer is built up any more, and the EM pulse radiates toward the Earth's surface as a free-field EM wave.

The equal speed for the gammas and E1 HEMP fields is important, because the EM field generated at a small position along the path might not be large, but there is a synchronized phasing effect. Now consider the next point along the path (the process really happens continuously along the path, not in discrete points – it is just easier to think of it in terms of discrete positions along the burst-to-observer path). At this point the process repeats, and more EM field is generated, to propagate toward the observer on Earth – and this new EM field adds onto the EM field that is already propagating by from the previous generation point. This is what is meant by "phased generation" – along 10's of kilometers of path length we have EM fields generated, and these travel down toward

the observer – each adding onto, and strengthening, the EM field that is also passing by from previous generating points along the path already traveled from the burst point. The build-up of the E1 HEMP is represented by the increasingly larger E-H-P vectors in the figure.

Eventually almost all of the gammas will have been attenuated by going through the air (especially with the ever-increasing air density further down in altitude), and there is no more generation and incremental increase of the EM signal. However, the EM signal continues on, heading toward the observer on the Earth. Just as the gammas were a spherical shell moving away from the burst point, the E1 HEMP is also a spherical shell (although, it turns out, not as thin as the few meters of the gamma shell). Air does not significantly attenuate EM fields for the frequencies of HEMP, and so this shell propagates on toward the Earth's surface with only the 1/r (for field strength) spherical divergence.

Historically this primary signal from the E1 HEMP has been called the "dipole term" (or more precisely, "magnetic dipole term") because of the spatial variation of the signal strength – variation of observer position relative to the geomagnetic field line direction.

So, in summary, the gammas generate forward-going source electrons that get turned by the geomagnetic field, producing a transverse current. This current radiates a forward-going EM wave. This occurs all along the ray path through the source region, with a little more EM field added onto the total E1 HEMP signal at each point. This is exactly the same effect as a phased array antenna (except without the frequency sensitivity of the antenna). Such an antenna has several emitting elements, with each sending out an EM wave. For the desired direction and frequency, the signals from each array element have just the right delay so that their oscillatory EM waves perfectly match up, and add together. This phased array build-up is a well-known effect in antenna theory.

Figure 4-3 pictorially shows the E1 HEMP generation process for the dipole term. The top of the left column shows the Compton scatter and forward current. This results in the forward source current and electric field shown below in that column. This E field is not the E1 HEMP (although it cannot be completely ignored in calculations, due to "self-consistency" effects, as we shall see). The next column shows the Compton electrons being turned in the geomagnetic field (represented by the blue "B" vector). This produces electron motion, and an electric field, that is perpendicular to the forward direction and to the geomagnetic field, as shown in the lower box of that column. However, there is another mechanism, and that is induced air conductivity. All the energy being dumped into the air causes a huge quantity of free electrons to eventually be produced, and those electrons then travel in the opposite direction of the electric field terms, as shown in the top of the last column. Then, as shown below that, these conduction currents are oriented in the opposite direction to the original source currents, and thus work against generation of the E1 HEMP field. The green line in Figure 4-4 represents an E1 HEMP that might result if there was no air conductivity. The blue line is a limit imposed by there really being air conductivity, and the red line shows the actual E1 HEMP for this case.

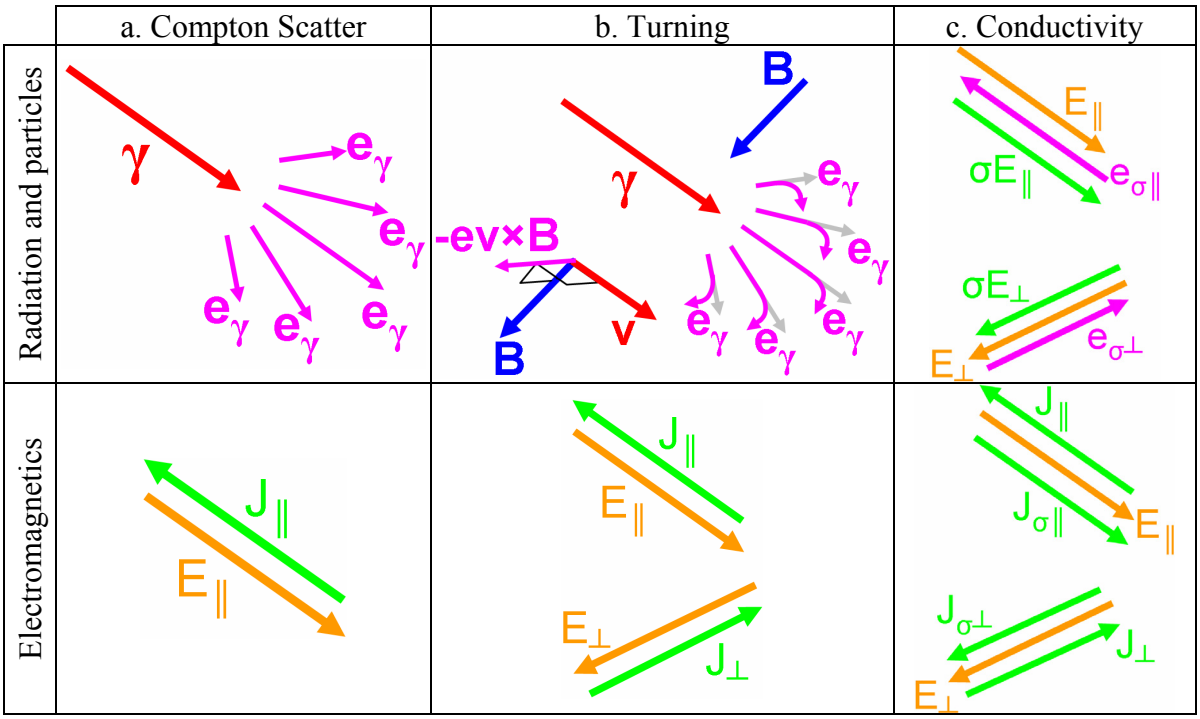

Figure 4-3. Details of the E1 HEMP generation in the source region. Drawing "a" shows the initial Compton scattering, producing a forward (on average) electric source current, which generates a local E field parallel with the burst-observer ray direction. In "b" the Compton electrons come under sideway force due to the motion of their charge in the geomagnetic field. The turning component of their motion is perpendicular to both the geomagnetic field and their forward motion. (The Earth's magnetic field points downward, at the local dip angle, in the northern hemisphere.) In column "c" we show conduction current. As a significant amount of lower energy secondary electrons are produced, air conductivity (σ) is produced, resulting in air currents (σE) directed against the source current.

Looking back at Figure 4-2 again, we show the electrons as having curved paths, not just being turned in only the transverse direction. This is a well-known effect – electrons actually tend to spiral around the B field lines. This is because the initial turned direction is, by construction, exactly perpendicular to the geomagnetic field, and so there is further turning force on the electrons. This leads to another source current term, and another electric field term. This additional term has been traditionally called the quadrupole (or more precisely, electric quadrupole) term. We will discuss this more later.

Finally, Figure 4-5 shows a hypothetical laboratory experiment that might show the E1 EMP generation process. There is a column of air, at the pressure of about the 20 km altitude, with a gamma source shining a beam from the left. We have shown a vacuum on the left, but only because it does not matter if it is air or vacuum there – we assume the air column is thick enough that all the gammas and Compton electrons cannot make it through this column. Also within the column is a magnetic field. An EM field should be emitted out the right side. However, no such test has been done – such a test is not practical – the air column would need to be much too wide to fully simulation E1 HEMP generation.

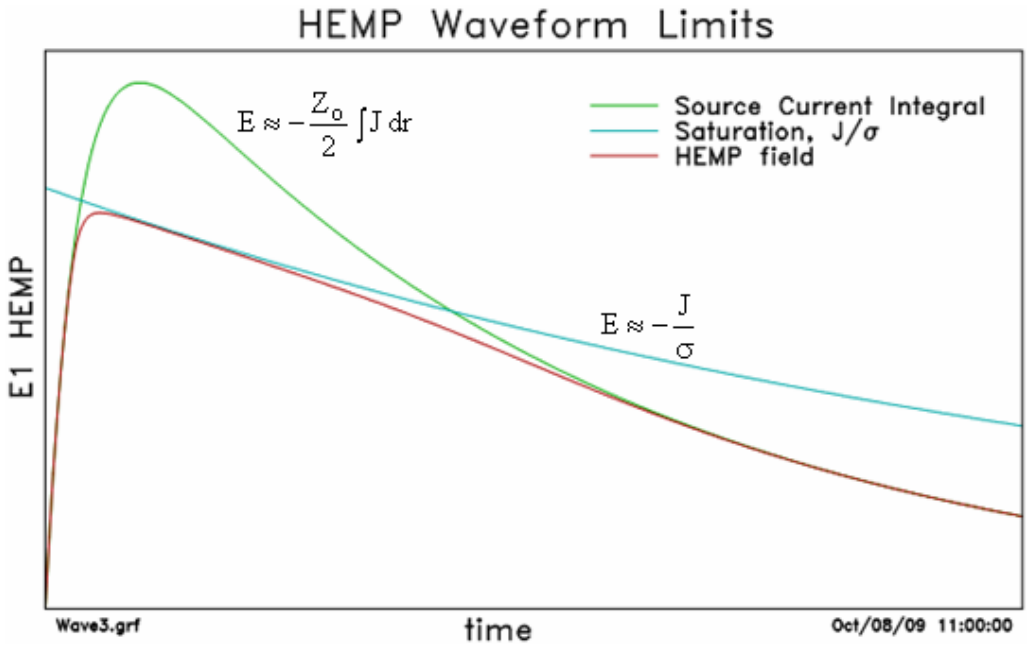

Figure 4-4. Representation of the generation of E1 HEMP. The green line, which has the shape of the incident gamma pulse, shows the electric field if no conductivity is generated. However, conductivity will be generated, and the red line shows the actual E1 electric field – it initially follows the no-conductivity field. However, as the conductivity builds up it gets limited by the saturated electric field, in blue. Later, the driven electric field (green line) has fallen below the saturated field, and starts to follow the red line again.

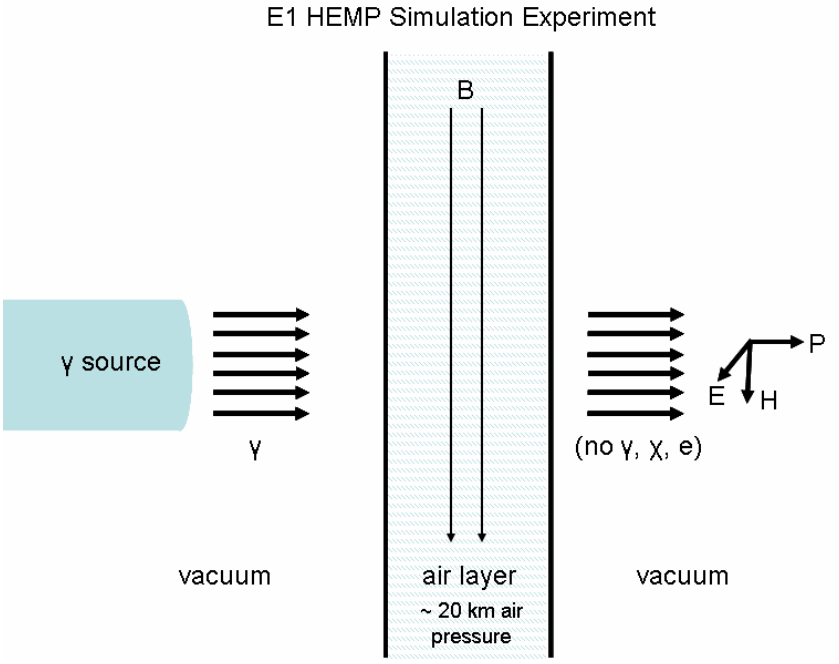

Figure 4-5. Laboratory E1 HEMP generation experiment. This shows an example of a hypothetical laboratory demonstration of the E1 HEMP generation process. A plane wave of gammas is incident on a planar sheet of air, in which there is also a static magnetic field. On the other side of the target sheet of air there is a radiated EM field (to either side of the air sheet there is vacuum, although it could also be air for the right side). Unfortunately, the gamma cross section for air is such that the sheet of air would need to be many kilometers thick to create such as laboratory demonstration.

This is a very complex process, and much effort was put into trying to characterize it for EMP studies. A high energy Compton electron gradually loses energy as it repeatedly collides with an air molecule. Each such collision results in an additional freed electron (a secondary), and some loss of energy for the original Compton electron. Typically there is about one initial secondary electron created (one collision) for each 85 eV of energy loss from the Compton electron. Each secondary electron generally has on the order of 10's of eV of energy. However, a few do have higher energies, enough to go on and have more ionizing collisions themselves, producing more freed electrons. It has been found that, after all the higher energy electrons have lost their excess energy, the final set of freed electrons have on the order of 10 eV of energy, and there is about one of these freed electrons produced for each 34 eV of energy lost by the initial primary electron. For a 1 MeV Compton electron this is about 30,000 conduction electrons.

The exact process of the build up of freed electrons by a Compton electron is very important, since more delay generally means higher E1 HEMP levels. The initial Compton electron starts building the E1 HEMP electric field level higher as it turns in the geomagnetic field, while it randomly also starts colliding with air molecules. These collisions happen over some time frame, and involve two effects that diminish the E1 HEMP level. The collisions impede the forward motion of the Compton electron, thus reducing the source current. Also, the collisions generate secondary electrons, contributing to air conductivity, and shorting out of the electric field. The secondary electrons also, over time, lead to more electrons (about 85eV/34eV = 2.5 final electrons per each 85 eV of energy lost). There are time evolutions for these effects, and details of these processes, especially delays to the processes, affect the E1 HEMP level.

Once freed electrons are generated, the "air chemistry" processes come into play. A freed electron does not stay free forever, as there are various processes that work to remove electrons. General EMP studies (for all burst altitudes) account for free electrons, and positive and negative ions (charged air molecules). A free electron can become attached to a neutral oxygen molecule in the two-body process

$$e + O_2 \rightarrow O^- + O \qquad (\text{rate constant } k_1) \quad .$$

Here we show that there is a rate constant that governs how quickly this process can occur. The air chemistry rate constants have values that depend on the air density and electric field. The electric field is important because it affects the average velocity of the conduction electrons – the electrons move under the force of the electric field and accelerate to higher speeds with higher E field. The air density is also important – the lower the air density, the more time between collisions, and so the higher the electron velocity when it finally does collide. Air density also governs the likelihood of a collision – the more air molecules there are to hit, the more likely there is a collision. (This is even truer when it is a three-body collision, such as for SREMP; then the rate constant variation goes as the square of the air density.)

A second air chemistry reaction is dissociative recombination – a freed electron is absorbed by, and neutralizes, a positive air ion, which then splits into separate atoms

$$\begin{aligned} e + O_2^+ &\rightarrow O + O \\ e + N_2^+ &\rightarrow N + N \end{aligned} \qquad \text{(rate constant } k_2\text{)} \quad .$$

Air molecule ions are created when an electron is knocked free (making a positive ion) or when an electron attaches (making a positive ion). These ions can recombine, and neutralize, in a two-body reaction such as

$$\begin{aligned} O_2^- + O_2^+ &\rightarrow O_2 + O_2 \\ O_2^- + N_2^+ &\rightarrow O_2 + N_2 \end{aligned} \qquad \text{(rate constant } k_3\text{)} \quad .$$

Usually EMP studies use the same k_2 and k_3 rate constants for nitrogen and oxygen, since little difference has been found in their values for these two types of molecules.

The air chemistry equations account for the various reactions just discussed:

$$\frac{dN_e}{dt} = S_e + k_a N_e - k_1 N_e - k_2 N_e N_+$$

$$\frac{dN_+}{dt} = S_e + k_a N_e - k_2 N_e N_+ - k_3 N_+ N_-$$

$$\frac{dN_-}{dt} = k_1 N_e - k_3 N_+ N_-$$

where "N" are densities of the charged species (electrons and ions), "Se" is the production rate of free electrons (which drives the equations), and the "k" values are the rate constants already introduced (these are functions of electric field and air density). As noted, the free electrons generally are created with energies of tens of eVs. Once they have participated in the conductivity for a while they tend to have energies governed by the electric field level and the air density (spacing between collision targets). If the electric field is high, and the air density low enough, an electron can build up substantial energy in its travels between collisions – high enough energy to even have an ionization collision, and so generate an additional freed electron. This is, appropriately, called avalanche. It represents another source of conduction electrons besides the collision loss of energy from the primary Compton electrons. We use "k_a" for the avalanche rate constant. Its value is higher for stronger E field and lower air density. It gives the average number of ionizations per freed electron, for a unit of time.

In EMP studies, the air chemistry equations are used to account for the reactions above, including avalanche, and so to calculate the numerical value for the number density of charged species at any time and position: freed electrons, positive ions, and negative ions (as stated, ignoring whether the ions are oxygen or nitrogen). These numbers are then used to calculate air conductivity.

In Maxwell's equations the conduction current is represented by a conductivity "σ", so that the conduction current is proportional to the electric field

$$J_\sigma = \sigma E \quad .$$

The conduction current is also given by the net flow of the free electrons

$$J_\sigma = -e N_e v_e$$

where "e" is the electric charge, "N_e" is the density of free electrons, and "v_e" is their average velocity. As stated above, each electron's acceleration, and so its average velocity, is proportional to the electric field. EMP studies usually use a parameter called "mobility" to account for the process of electrons being accelerated in, and having collisions in, air. Electron mobility, μ_e, is the ratio of average velocity to driving electric field

$$\mu_e = \frac{-v_e}{E} \quad .$$

Conductivity can then be written as

$$J_\sigma = \sigma E = -e N_e v_e \quad \rightarrow \quad \sigma = \frac{-e N_e v_e}{E} = e N_e \mu_e \quad .$$

thus using number density and mobility. The same approach is used for the ions, positive and negative, so that the final air conductivity is taken to be

$$\sigma = e\left(N_e \mu_e + N_- \mu_- + N_+ \mu_+ \right)$$

where, as stated before, the mobility values are essentially the same for oxygen and nitrogen, so we combine them both into total negative (N_-) and positive (N_+) ion densities. Actually, the mobility values are about the same for both polarities of ions also, so typically the conductivity just groups all ions ("I") together, giving

$$\sigma = e\left(N_e \mu_e + N_I \mu_I\right) .$$

The air chemistry rate constants and mobilities are functions of air density and electric field. Lower air density means more acceleration time between collisions, and higher electric fields mean more acceleration force. Also, water vapor means having water molecules present in the air too, and this can have significant effects on the parameters. However, water vapor is often not considered very important for the high altitudes of E1 HEMP generation.

E1 HEMP is only concerned with very early times, and low air density. This means that typically the ions are ignored, as their levels have not yet built up enough to be significant. Thus, only the attachment and avalanche processes are considered.

Studies to characterize the air conductivity processes have been a significant part of E1 HEMP efforts. Air chemistry is especially important for predicting peak field levels, because of the competition between Compton and conduction currents. Anything that could delay the air conductivity could lead to significantly higher field levels. One process of concern involves the electrons freed when a Compton electron collides, and the fact that there is some excess energy that eventually produces more ionization (the extra ~1.5 free electrons per initial secondary). It is important to accurately account for the higher energy secondary electrons. However, in the lab we can only study them indirectly, as we do not have a good method of experimentally simulating E1 HEMP directly.

A major potential source of uncertainty for E1 HEMP calculations is due to various aspects of air conductivity. One aspect of this is that the E1 HEMP peak level depends on how fast the air conductivity turns on. This can be very critical for fast gamma pulses

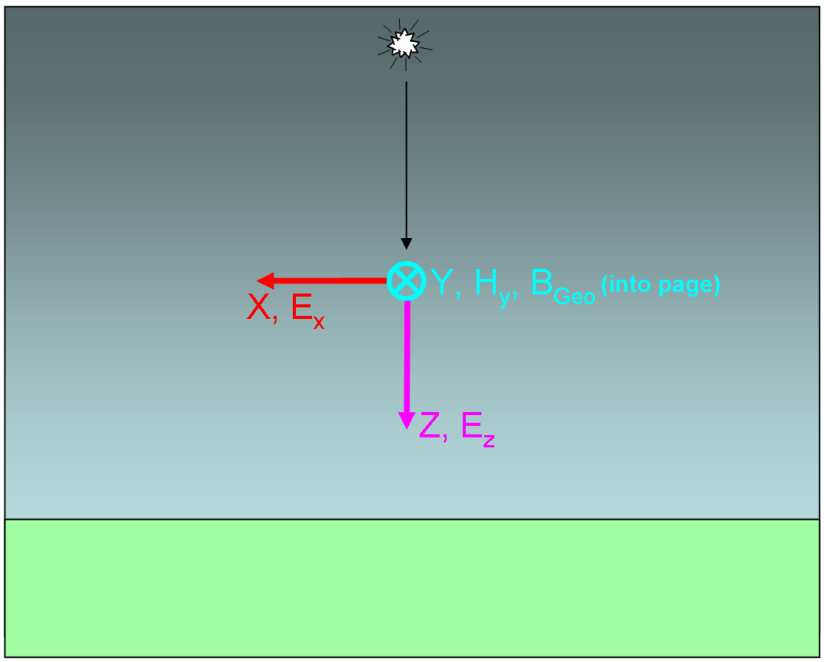

Figure 4-10. Terms and vector directions for the E1 HEMP equation derivation.

Maxwell's equations for the case are:

$$\mu_o \frac{\partial H_y}{\partial t} = -\frac{\partial E_x}{\partial z}$$

$$\varepsilon_o \frac{\partial E_x}{\partial t} + \sigma E_x + J_x^c = -\frac{\partial H_y}{\partial z}$$

$$\varepsilon_o \frac{\partial E_z}{\partial t} + \sigma E_z + J_z^c = 0 \ .$$

Besides the fields already mentioned, there is the source currents from the initial Compton electrons (J_z^c) and from their turning (J_x^c). There is also air conductivity (σ), which builds up from the energy loss of the Compton electrons.

Next some transformations of variables are used. The first is the use of "retarded time"

$$\tau = ct - z$$

which is a time scale that is synchronized with waves (the gammas and electromagnetic fields) moving downward with the speed of light. The other transformation replaces two of the field components with

$$F = E_x + Z_o H_y$$

$$G = E_x - Z_o H_y$$

where "F" is the outward (or downward) going wave, and "G" is the inward (or upward) going wave. F will become the E1 HEMP that propagates down to the Earth. The traditional fields can be reconstructed from

$$E_x = \frac{F+G}{2}.$$

$$H_y = \frac{F - G}{2 Z_o}.$$

With the retarded time transform the derivatives change as

$$\frac{1}{c}\frac{\partial}{\partial t} \rightarrow = \frac{\partial}{\partial \tau}$$

$$\frac{\partial}{\partial z} \rightarrow \frac{\partial}{\partial t} - \frac{\partial}{\partial \tau}.$$

And putting in the inward and outward waves, Maxwell's equations become:

$$\frac{\partial F}{\partial z} + \frac{\sigma Z_o F}{2} = -Z_o J_x^c - \frac{\sigma Z_o G}{2}$$

$$\frac{\partial G}{\partial \tau} + \frac{\sigma Z_o G}{4} = -\frac{1}{2}\frac{\partial G}{\partial z} - \frac{Z_o J_x^c}{2} - \frac{\sigma Z_o F}{4}$$

$$\frac{\partial E_z}{\partial tz} + \sigma Z_o E_z = -Z_o J_z^c.$$

These are exact transforms of Maxwell's equations given above – no approximation has been applied.

Note that the equations are separated into sets. The third only involves E_Z and J_Z and is independent of the first two. This is just the local electric field (with no associated magnetic field), due to the separation of charge produced by the Compton scattering knocking electrons in the forward direction. This does not propagate away from the source region. We can ignore E_Z for the rest of this discussion. It is, however, important when doing a full calculation of E1 HEMP, because of self-consistency: the electric field acts on the Compton electrons, thus affecting the source current, and also affects the average energy of conduction electrons, which in turn affects parameters in the "air chemistry" used to calculate air conductivity.

For very early time the air conductivity has not built up yet, so those terms can be dropped, and the remaining E1 HEMP equations become

$$\frac{\partial F}{\partial z} = -Z_o J_x^c$$

$$\frac{\partial G}{\partial \tau} = -\frac{1}{2}\frac{\partial G}{\partial z} - \frac{Z_o J_x^c}{2}.$$

The first one shows that the forward wave starts to build up as

$$F(z,\tau) \cong -Z_o \int_0^z J(z',\tau)\,dz' \quad .$$

As the conductivity and electric field build up, the conduction current (σE) can become significant, and if it dominates, the first equation instead is approximately

$$\frac{\partial F}{\partial z} + \frac{\sigma Z_o F}{2} = 0$$

where we have also assumed that the upward wave, G, is not significant. Under these conditions the forward wave is given by

$$F(z,\tau) \cong -\frac{2\,J(z,\tau)}{\sigma(z,\tau)} \quad .$$

This is the saturation condition. Except for very low gamma output bursts, or very far distances from the burst (such as high HOB), saturation typically does occur. It tends to limit the strength of E1 HEMP. It is also the reason that, even with more than three orders of magnitude variation in burst total yield, the values of the largest E1 HEMP field from nuclear bursts have much less variation.

Now consider the upward going wave, G. The downward wave (F), with only a spatial derivative in z (altitude), builds up over distances of about a scale height of the exponentially increasing air density (scale height is the distance over which the atmosphere density changes by an e-folding, e^{-1}, and is about 7 kilometers in the lower atmosphere). However, the outward wave (G) equation has a retarded time derivative, and this dominates. This represents a wave buildup over the retarded time width of the pulse, which is only a few meters – much shorter than the build-up distance for the F term. This means G is much smaller than F. For example, a 50 nanosecond pulse has a spatial width of 15 meters ($c\,\Delta t = 3\times10^{8} * 50\times10^{-9} = 15$ meters). With the insignificant spatial derivative removed, the G equations becomes

$$\frac{\partial G}{\partial \tau} + \frac{\sigma Z_o G}{4} = -\frac{Z_o J_x^c}{2} - \frac{\sigma Z_o F}{4} \quad .$$

Thus the upward wave is driven by the turned current and F's conduction current (the drivers on the right side of the equations), while air conductivity resists the build-up of G (just as for F; the σG on the left side). However, if there is saturation of the F term, then, as discussed above, the current and F are directly related as

$$J_x^c \cong -\frac{\sigma F}{2} \quad .$$

Then the driver term (right hand side) for G then becomes

$$\frac{Z_o J_x^c}{2} + \frac{\sigma Z_o F}{4} \cong 0$$

thus the driver for G is zero, and so this is another reason for G not getting big. Thus G does not build up to any significant level

$$G \cong 0 \quad .$$

With G zero, the transformations then give

$$F \cong 2E_x$$

$$E_x \cong Z_o H_y \quad .$$

The second equation is that of a propagating electromagnetic plane wave.

Going back to Maxwell's equation for F (with G=0) and transforming back to the electric field term, we get

$$2\frac{\partial E_x}{\partial z} + \sigma Z_o E_x = -Z_o J_x^c \quad .$$

This is the standard E1 HEMP result – it is called the outgoing-wave approximation, or the high-frequency approximation. The early time approximate solution for this is

$$E_x \cong -\frac{Z_o}{2}\int_0^z J_x \, dz' \quad .$$

(Karzas and Latter's corresponding spherical geometry result is

$$E \cong -\frac{Z_o}{2r}\int_0^r r' J \, dr' .)$$

and the saturated field approximation result is

$$E_x \cong -\frac{J_x}{\sigma} \quad .$$

These equations can be used to explain E1 HEMP, and check results, but computer code modeling of E1 HEMP usually uses the full set of Maxwell's equations. This is needed to include self-consistency – the electromagnetic field effects on the source currents and air conductivity.

Standard E1 HEMP codes use retarded time and inward/outward going waves, as shown in the initial part of the derivation above. However, usually such codes are also "self-consistent", which means:

1. The Compton electrons respond to the force of the local electric and magnetic fields generated by the nuclear output (they do not just respond to the geomagnetic field).
2. The air chemistry parameters are allowed to be functions of the electric field.

Thus, the upward going wave, which is part of the total fields in the source region, is not ignored. For computer solutions, the only approximation used for Maxwell's equation is ignoring the spatial derivatives with angle.

As mentioned before, for E1 HEMP typically the air chemistry is simplified by only accounting for the electrons (ignoring ions), so that the only air chemistry equation used is

$$\frac{dN_e}{dt} = S_e + k_a N_e - k_1 N_e \quad .$$

And then the air conductivity is calculated as

$$\sigma = e N_e \mu_e \quad .$$

Finite differencing is used for the air chemistry equation – calculating the free electron density with S_e as the producer of free electrons from energy loss of the Compton electrons; k_1 is the rate for attachment to neutral air molecules, and k_a is for avalanche. A major difficulty is determining the free electron source term, S_e.

The other difficult part is defining the source current, J. In simple terms the source is the sum of the velocity of all the Compton electrons in a unit volume, times the electron charge (a negative value). To use this, we need to account for Compton electrons. In the codes this is done by using "macroparticles". Compton electrons are sent out in all directions (although, on the average in the forward direction). The Compton electrons have different initial energies (correlated with scattering angle), and are affected differently according to their motion relative to the forces of the local electric and magnetic fields. But we cannot model each single electron. Instead we divide the scatter space into bins, and group all the Compton electrons within each bin into a single electron (a macroparticle) that represents, on average, all the electrons in that initial bin. Thus, for each time point (using finite difference), there might be 10 to 20 macroparticles that are generated. The code then follows each particle forward in time. A true electron would have random scatters through time and space, plus the acceleration/deceleration of the electric field, and turning by the magnetic field. For the macroparticles the random effects are put into an average behavior instead.

With this approach, the source current is simply

$$J = e\sum N_C v_C$$

where N_C represents the weight of each macroparticle, indicating how many Compton electrons each one represents. The weight values vary with the time waveform of the burst's gamma output, and the amplitude of the gammas that have not been scattered in getting to the position (all simple analytic calculations). However, for extra accuracy, generally there is also a factor included to help account for gammas that may have gone through small angle scatters (gammas with large scatters would be delayed too much in time to be of interest for E1 HEMP).

The macroparticles are governed by the relativistic equations of motion (using finite differencing). Also, Bethe's formula for average energy loss is used. This is a "drag force" for the motion – the particles slow down with the loss of energy associated with the Compton electrons scattering many times. Such scattering also represents some randomization in their motion, which lessens their forward motion (and so the Compton source current). This is handled by an approximate approach termed the "obliquity factor". All of this is calculated in retarded time, which requires care in setting up the equations.

The energy loss (Bethe drag) is also used to increase the electron density – as a source of one new freed electron for each 85 eV of lost energy. Although, as noted, eventually 1.5 more electrons will be freed per each initial electron. The timing of this generation of additional ionization has been studied, and a fit developed for the processing. The term "formative time lag" is associated with this. The waveform of the extra ionization has been fit to simple differential equations, so simple finite differencing may be used in the computer calculation to account for it.

The air chemistry equation for the electron density is carried forward with finite differencing. Analytic fits to experimental data are used to determined rate constants and electron mobility. From these, the air conductivity is calculated, and, with the source

current, the finite differenced Maxwell's equations can be advanced in time and space (down the ray).

4.4 E1 HEMP Decomposition

In this section we discuss E1 HEMP signals in a way that is both illustrative and useful. We derive a result that decomposes E1 HEMP so that some functional variations are readily seen. This derivation does not provide a way to calculate E1 HEMP directly, but its usefulness will become apparent. Initially we will just consider the early part of E1 HEMP, when conductivity can be ignored. Previously we showed that the field is approximately

$$\bar{E} = -\frac{Z_o}{2}\int \bar{J}\, dz \quad .$$

We will approximate the integral as the Compton current times some representative length, Δz

$$\bar{E} = -\frac{Z_o}{2}\bar{J}\,\Delta z$$

where J is the turned source current.

Now consider the turned current. The Lorentz force on an electron is given by its charge (e), velocity ($\bar{v}_0$), and the magnetic field (B – such as the geomagnetic field). This force causes acceleration of the electron (of mass "m") in the turned direction, leading to turned velocity $\bar{v}_1$

$$\bar{F}_1 = -e\left(\bar{v}_0 \times \bar{B}\right) = m\frac{d\bar{v}_1}{dt} \quad .$$

So that the turned velocity is

$$\bar{v}_1 = -\frac{e}{m}\int\left(\bar{v}_0 \times \bar{B}\right)dt$$

$$= -\frac{e}{m}\left(\bar{v}_0 \times \bar{B}\right)\Delta t$$

$$= -\frac{e}{m} v_0 B_{Geo}\,\Delta t\,\left(\hat{r} \times \hat{b}\right)$$

where we are using unit vectors (lower case, with "hats" above) to represent the direction of the various vector quantities

$$\bar{v}_0 = v_0\,\hat{r}$$

$$\bar{B} = B_{Geo}\,\hat{b}\,.$$

As before, we have simply replaced the integral by some representative time, Δt. The total turned current is given by the number of Compton electrons, N, their velocity, and the electron charge

$$\bar{J}_1 = -e\,N\,\bar{v}_1$$

$$= e\frac{e}{m} N\, v_0\, B_{Geo}\,\Delta t\,\left(\hat{r} \times \hat{b}\right).$$

Thus the turned current is proportional to the number and forward velocity of the Compton electrons, the geomagnetic field strength, and the cross product of the ray direction and B field direction. This cross product gives a direction, perpendicular to the ray and B, and an amplitude given as the sine of the angle between those two vectors.

Using this current and the form of the initial electric field from the high-frequency approximation we get

$$\bar{E}_1 = -\frac{Z_o}{2}\bar{J}_1\,\Delta z$$

$$= -\frac{Z_o}{2} e \frac{e}{m} N\, v_0\, B_{Geo}\, \Delta t\, \Delta z \left(\hat{r}\times\hat{b}\right).$$

(This is the E1 HEMP dipole term.) As a reminder, Table 4-2 shows the polarity of turned quantities: electron velocity, electric field, and source current. These are formed from the vector from the burst to the observer (the ray, direction $\hat{r}$), and the geomagnetic field in the source region (direction $\hat{b}$). Note that the Earth's north pole is the "north seeking" pole, and so is the south pole of the Earth's magnetic field. The geomagnetic field polarity is such that the field lines point from the south to the north. Using the standard "right hand rule" for the cross product gives the source current direction; the opposite direction (from the minus sign), or "left hand rule", gives the source electron and electric field direction.

Table 4-2. Vector directions for turned quantities.

Positive Directions	
$-\hat{r}\times\hat{b}$	$\hat{r}\times\hat{b}$
Left hand rule	Right hand rule
v_e, E	J
$\hat{r}$ = direction from the burst to the observer.	
$\hat{b}$ = direction of the geomagnetic field (it points down in the northern hemisphere).	

Now we will consider the same process for the second turning. Remember that the first-turn electron will also see the geomagnetic field – in fact, by construction, it is automatically fully perpendicular to the geomagnetic field. The second turning force, driven by the first turn velocity, leads to acceleration and a 2nd-turned velocity, $\bar{v}_2$

$$\bar{F}_2 = -e\left(\bar{v}_1\times\bar{B}\right) = m\frac{d\bar{v}_2}{dt} \quad .$$

Thus the velocity is

$$\bar{v}_2 = -\frac{e}{m}\int\left(\bar{v}_1\times\bar{B}\right)dt$$

$$= -\frac{e}{m}\left(\bar{v}_1\times\bar{B}\right)\Delta t$$

$$= \left(\frac{e}{m}\right)^2 v_0 B_{Geo}^2 \frac{\Delta t^2}{2} \left(\left(\hat{r}\times\hat{b}\right)\times\hat{b}\right)$$
$$= \upsilon_2 \left(\left(\hat{r}\times\hat{b}\right)\times\hat{b}\right)$$

where we have again simply used a time Δt to represent the integration (as noted, we will not use this analysis to calculate E1 HEMP). The "υ_2" represents the amplitude of all the various factors shown, and the vector function gives the direction and a geometry factor. The first turning had an amplitude factor from the cross product $\left(\left|\hat{r}\times\hat{b}\right| = \text{the sine of the angle between those two vectors}\right)$, for the second turning the amplitude of the vector $\left(\left|\left(\hat{r}\times\hat{b}\right)\times\hat{b}\right|\right)$ also equals the same sine function – the extra "$\times\hat{b}$" simply represents a change in direction.

Again we can form the source current for the second turning

$$\bar{J}_2 = -e\,N\,\bar{v}_2$$
$$= -e\left(\frac{e}{m}\right)^2 N\, v_0 B_{Geo}^2 \frac{\Delta t^2}{2} \left(\left(\hat{r}\times\hat{b}\right)\times\hat{b}\right).$$

But before going further we should note that the high-frequency approximation uses the part of the source current that is perpendicular to the ray direction. We will also show that, unlike the first turning, only part of this current is perpendicular to the ray, and some is parallel to the ray (and this part does not radiate down the ray).

In general, a vector ($\bar{v}_2$) can be separated into a two parts, relative to another vector (the burst observer ray here, $\hat{r}$)

$$\bar{v}_{2||} = \left(\hat{r}\bullet\hat{v}_2\right)\hat{r} \qquad \text{(parallel)}$$
$$\bar{v}_{2\perp} = \left(\hat{r}\times\hat{v}_2\right)\times\hat{r} \quad \text{(perpendicular)}.$$

As noted, the parallel component does not radiate as part of E1 HEMP. We will only consider the important component (perpendicular), and put in its vector direction from the results above

$$\bar{v}_{2\perp} = \left(\hat{r}\times\hat{v}_2\right)\times\hat{r}$$
$$= \upsilon_2 \left(\hat{r}\times\left\{\left(\hat{r}\times\hat{b}\right)\times\hat{b}\right\}\right)\times\hat{r}$$
$$= \upsilon_2 \left(\hat{r}\bullet\hat{b}\right)\left\{\left(\hat{r}\times\hat{b}\right)\times\hat{r}\right\}.$$

The third line is the result of vector simplification, shown in Table 4-3. We will see that, compared to the dipole (E_D) term, this means that the quadrupole (E_Q) term has two extra geometry effects: an extra amplitude scaling from $\hat{r}\bullet\hat{b}$, and an extra direction change (by 90^o) from the last $\times\hat{r}$.

This same selection of the transverse component can be applied to the second-turned source current, so that the second-turned E1 HEMP field is

$$\bar{E}_{2\perp} = -\frac{Z_o}{2}\bar{J}_{2\perp}\Delta z$$

For damage it is actually the high end "tails" of the curves that are important – where the voltages get into the hundreds of kilovolts that could cause insulator or transformer damage. The probability is not high for the example shown – it can get higher for some cases. However, even a low probability can be a problem because, for example, there are many insulators along a power line, and any one of them failing can result in the loss of the whole line. It should be emphasized that the single device used here is not a least or a worst-case device, so the results are representative. In particular, the worst-case E1 HEMP used by the military in MIL-STD-188-125-1 for an E1 HEMP powerline current is 5,000 amperes. The characteristic impedance for a power line is approximately 400 ohms, thus providing a peak worst-case voltage level of 2 MV.

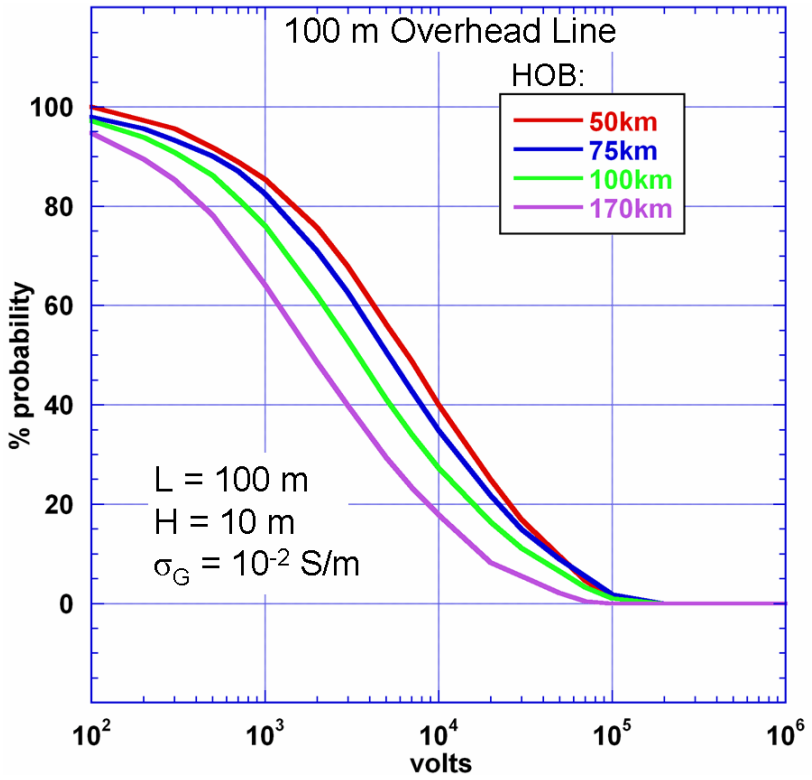

Figure 7-1. Voltage distribution for a 100-meter long horizontal power line. The results are for a typical burst, for four burst heights over the U.S. The power line is 10 meters over 10^{-2} S/m ground.

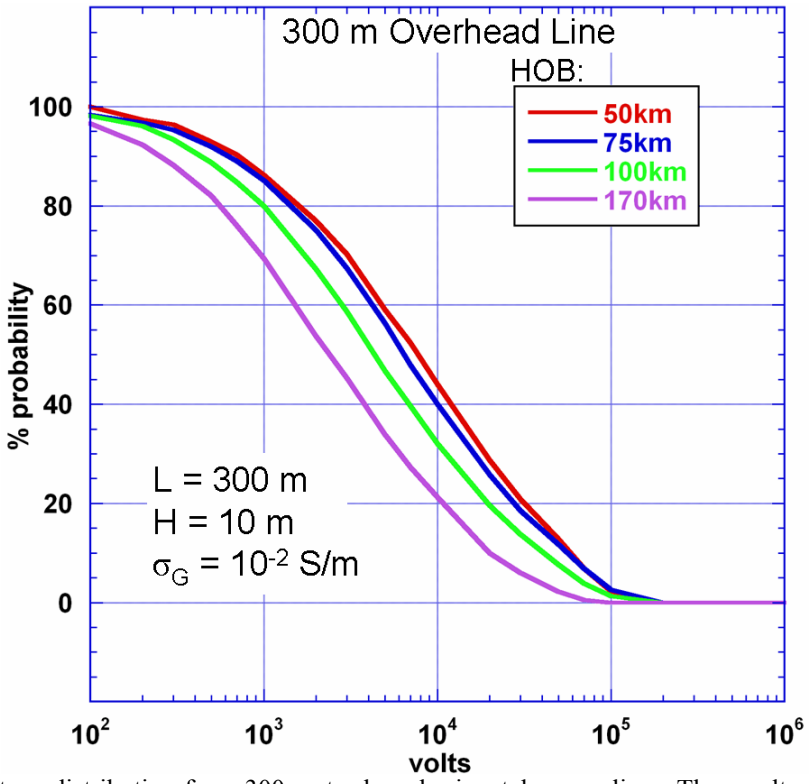

Figure 7-2. Voltage distribution for a 300-meter long horizontal power line. The results are for a typical burst, for four burst heights over the U.S. The power line is 10 meters over 10^{-2} S/m ground.

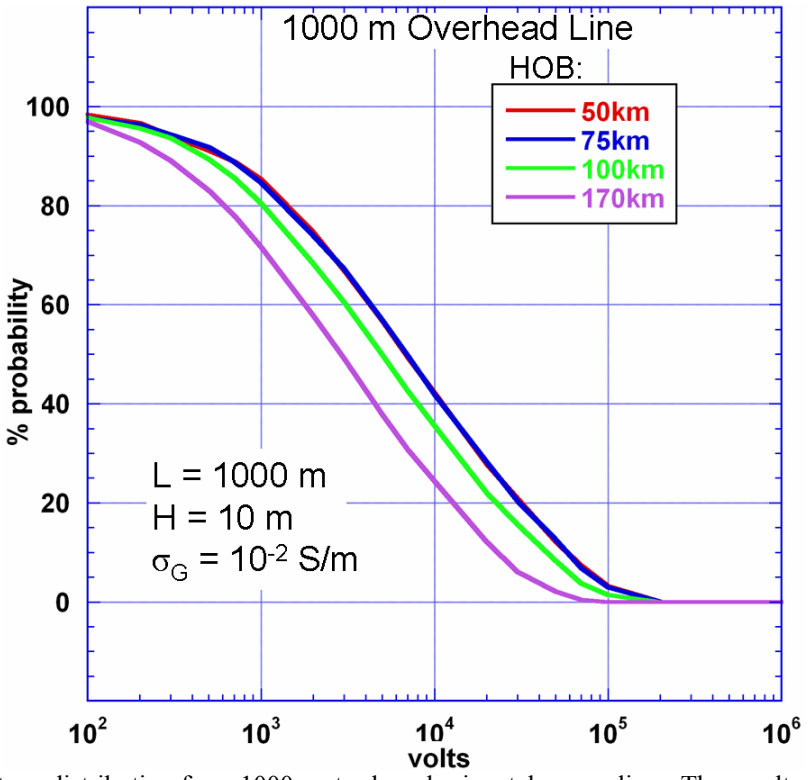

Figure 7-3. Voltage distribution for a 1000-meter long horizontal power line. The results are for a typical burst, for four burst heights over the U.S. The power line is 10 meters over 10^{-2} S/m ground.

Additional calculations are also presented for lines near the surface of the earth (on or slightly below), as these might represent control and sensor lines in a power substation. Shorter line lengths were used: 10, 30, and 100 meters. The next three figures (Figures 7-4 to 7-6) show these results – note that the voltage axis has lower values than for the power line. This is because the earth has the effect of reducing the propagation of the coupled HEMP voltages. For these cases the 75 km HOB does better than 50 km, but the 170 km case is still the result most to the left. The average voltages (50%) for the 10-meter length (Figure 7-4) are 130 V for 170 km and 350 V for 75 km. For the 100 m line length (Figure 7-6) the averages are 380 V for 170 km and 780 V for 75 km. These are less than the results for the 100 m overhead line because the line is closer to the ground. However, note that the distribution also shows that a fair fraction of the lines would have voltages up to thousands of volts. Also, these results are for lines run near the ground – coupling would be even stronger if the line runs are higher off the ground.

The last result (Figure 7-7) is for a vertical control/sensor line or feeder line that is only 4 meters long. However, the results are higher than the longer horizontal lines. The average voltage is 1200 V for the 170 km HOB, and 4000 V for the 50 km HOB. The higher values are due to the vertical field not being shorted out by the ground – it can actually be enhanced by ground reflection.

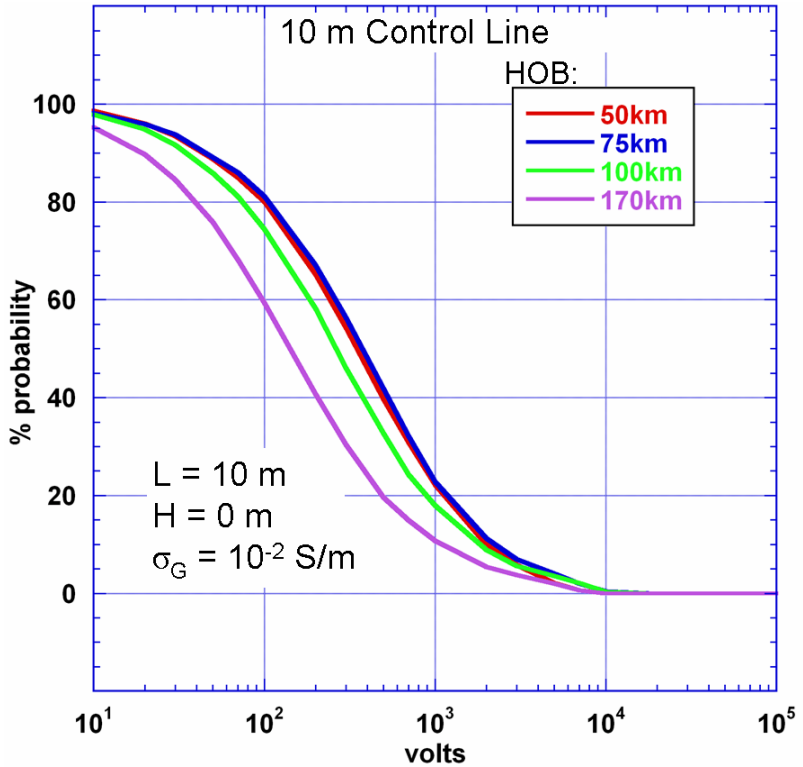

Figure 7-4. Voltage distribution for a 10-meter long horizontal control/sensor line. The results are for a typical burst, for four burst heights over the U.S. The line is lying on the surface of 10^{-2} S/m ground.

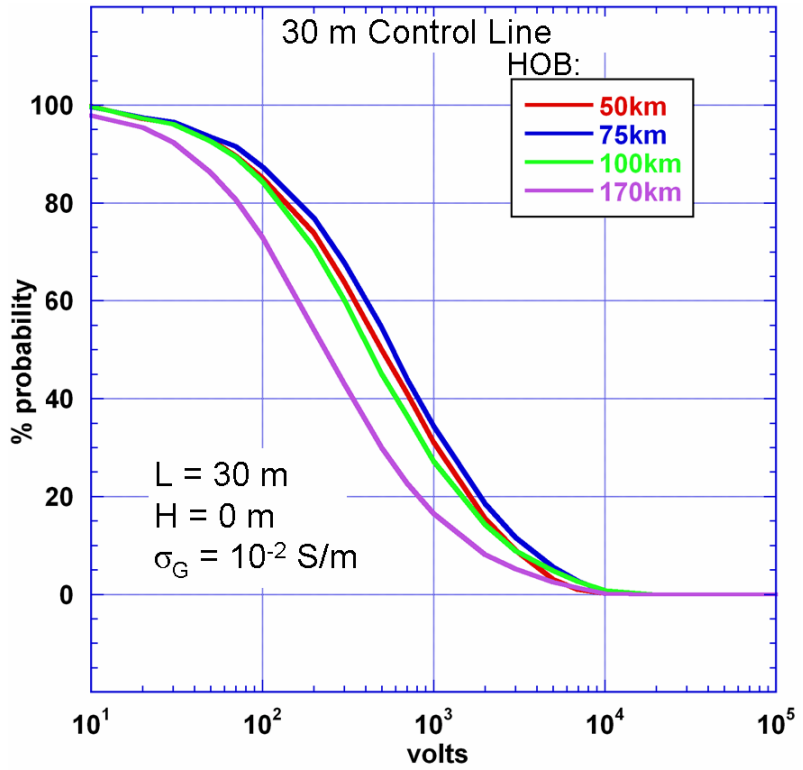

Figure 7-5. Voltage distribution for a 30-meter long horizontal control/sensor line. The results are for a typical burst, for four burst heights over the U.S. The line is lying on the surface of 10^{-2} S/m ground.

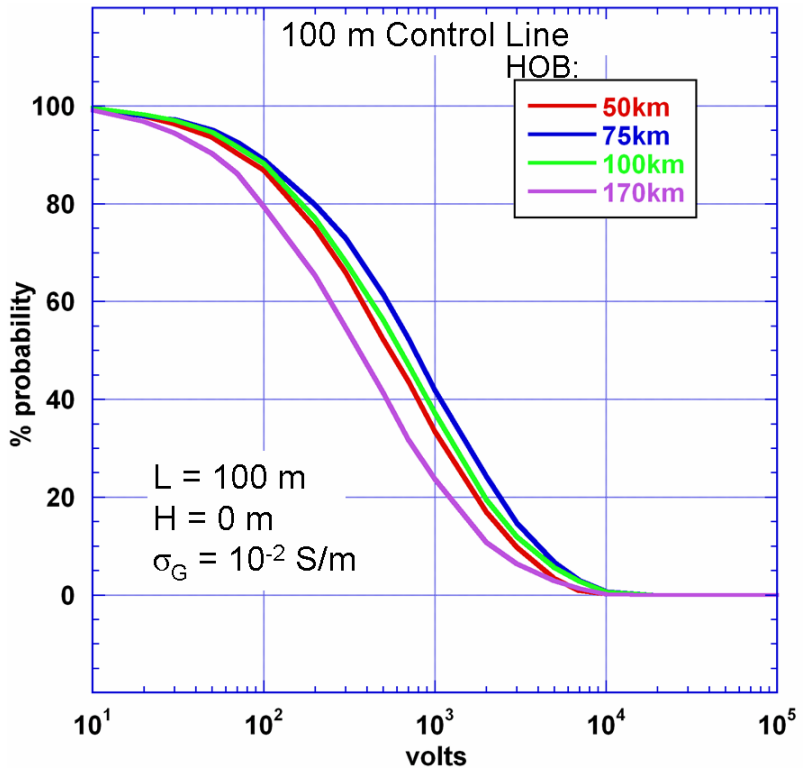

Figure 7-6. Voltage distribution for a 100-meter long horizontal control/sensor line. The results are for a typical burst, for four burst heights over the U.S. The line is lying on the surface of 10^{-2} S/m ground.

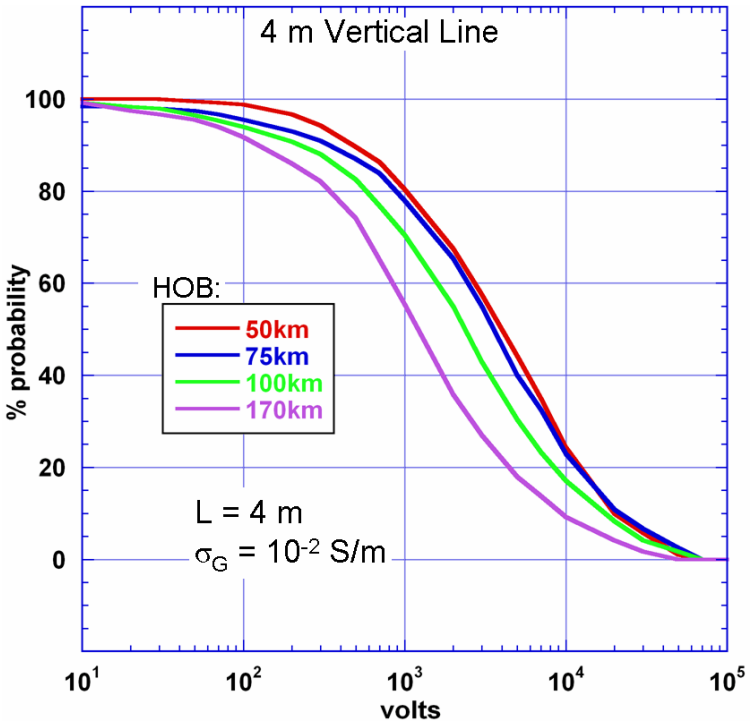

Figure 7-7. Voltage distribution for a 4-meter long vertical control/sensor line. The results are for a typical burst, for four burst heights over the U.S. The line extends upward from the 10^{-2} S/m ground.

7.2 Susceptibility of Power System Equipment

There have been various studies of the power grid vulnerability to E1 HEMP in the past, such as those listed in Table 7-2. Insulator flashover is a major vulnerability studied. Damage to distribution transformers has also been considered. Another concern is the ubiquitous use of electronic devices to control processes, including power substations, control centers, and generation stations.

In Section 7.1 calculations indicated that control/sensor/communication wires can have coupled E1 HEMP peak voltages of thousands of volts. Normally such lines transmit signals of a few volts, and so E1 HEMP pulses could certainly be disruptive. There are many electronic devices that are located in a power substation, central control facility, or generator station that would also have attached cables. These include:

1. Computers, of various kinds.
2. PLCs – programmable logic controllers – basically computers, but specialized with I/O ports, such as A/D and D/A converters (A= analog, D= digital) so that they can be process controllers.
3. Communication devices – modems, routers, switches, etc.
4. Solid-state safety relays (increasingly used as replacements for the older electromechanical power relays).
5. SCADA systems (Supervisory Control And Data Acquisition) – this involves communication of data and controls between unmanned substations and manned control centers.

Figure 7-16. Exposure area for E1 HEMP burst at 170 km over Ohio.

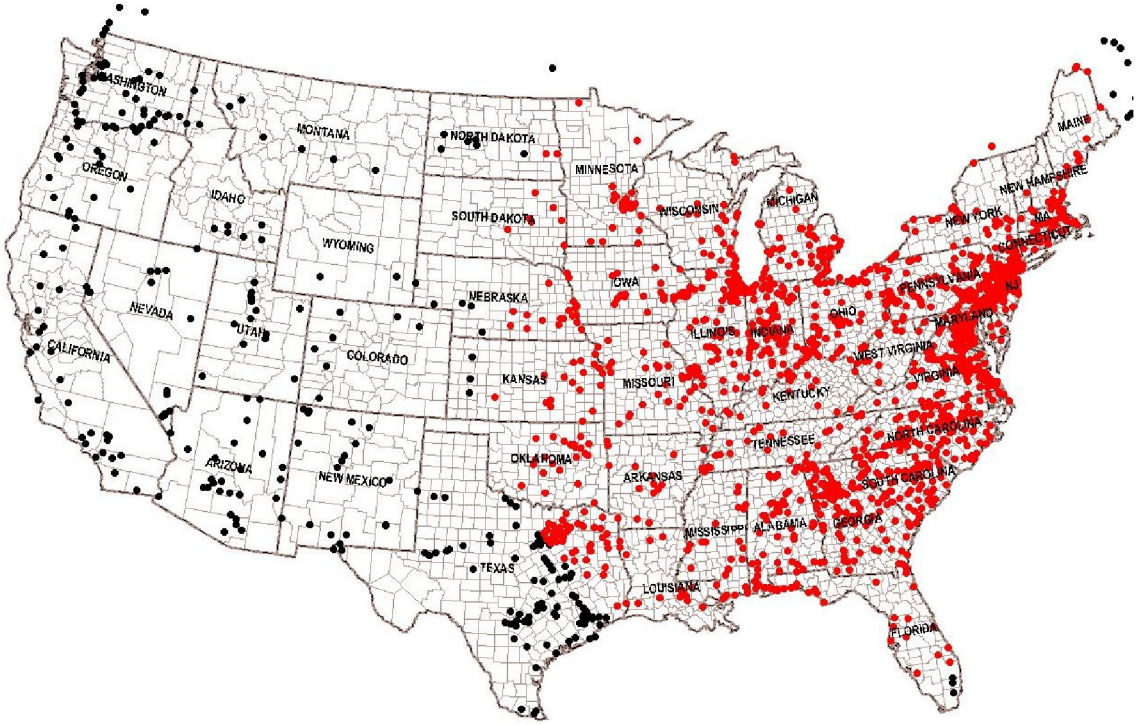

Figure 7-17. EHV substations in the exposed region shown in Figure 7-16. There are 1765 EHV substations exposed (red dots), about 83% of such substations for the country. (EHV indicates 345 kV or higher.)

The biggest E1 HEMP concern within a high voltage substation is not the high voltage transmission lines and transformers, but rather the low voltage sensor and control lines that extend from the transformer yard to the relays and other control electronics in the control building. While these cables are in conduits above ground (shown in Figure 7-18), these conduits are not effective electromagnetic shields at high frequencies. Currents and voltages coupled to an external conduit are likely to leak into the internal cable at the joints and at connection points to sensors and the controls.

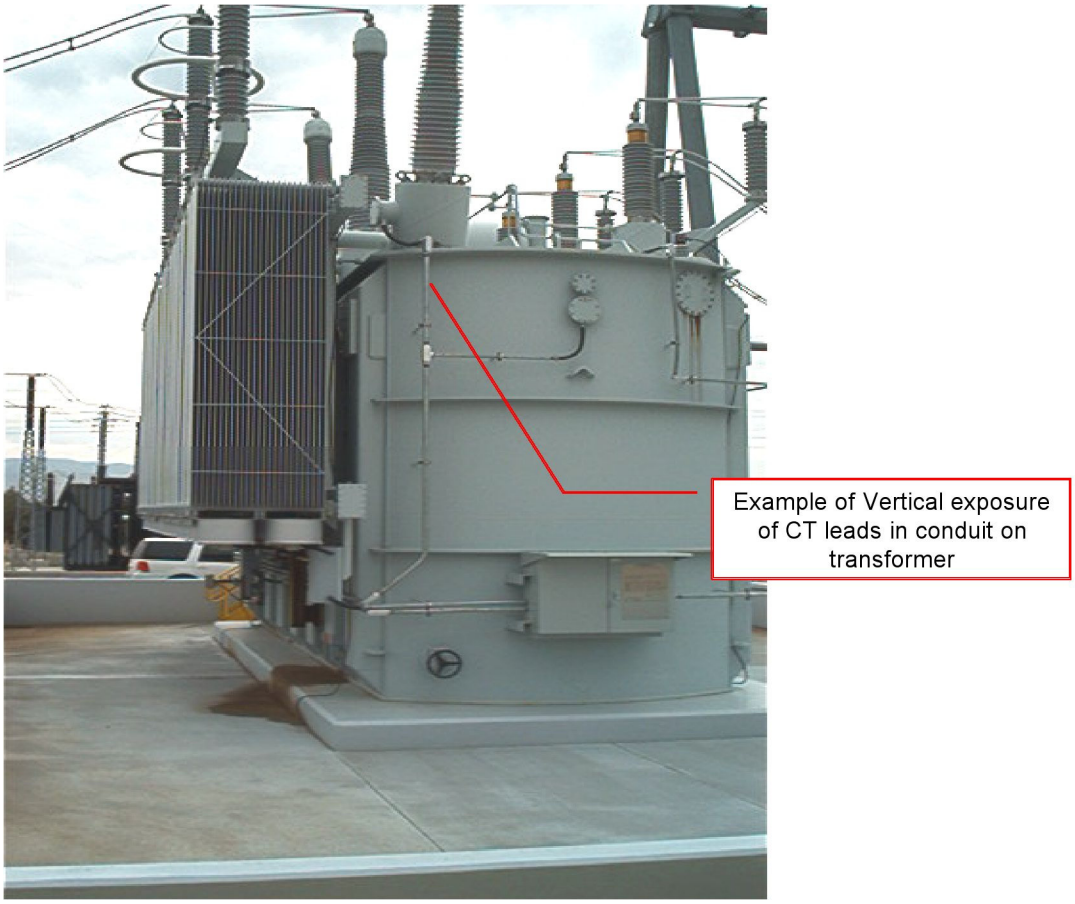

Figure 7-18. Exposure of cable conduits on transformers.

In Figures 7-19 and 7-20 the sensor and control cables are seen to run slightly below ground in trenways that are "buried" in the gravel in the transformer yard. The length of these cables and the poor electromagnetic shielding of the trenway and the gravel at high frequencies will allow the penetration and coupling of high frequency fields to the cables and the subsequent propagation of these currents and voltages to the control building.

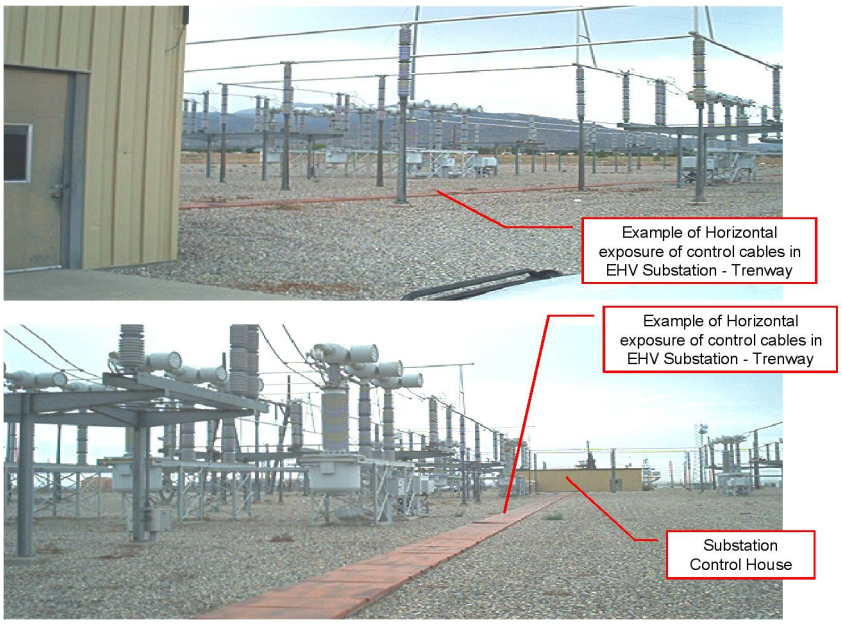

Figure 7-19. Long runs of "buried" cables in low conductivity gravel.

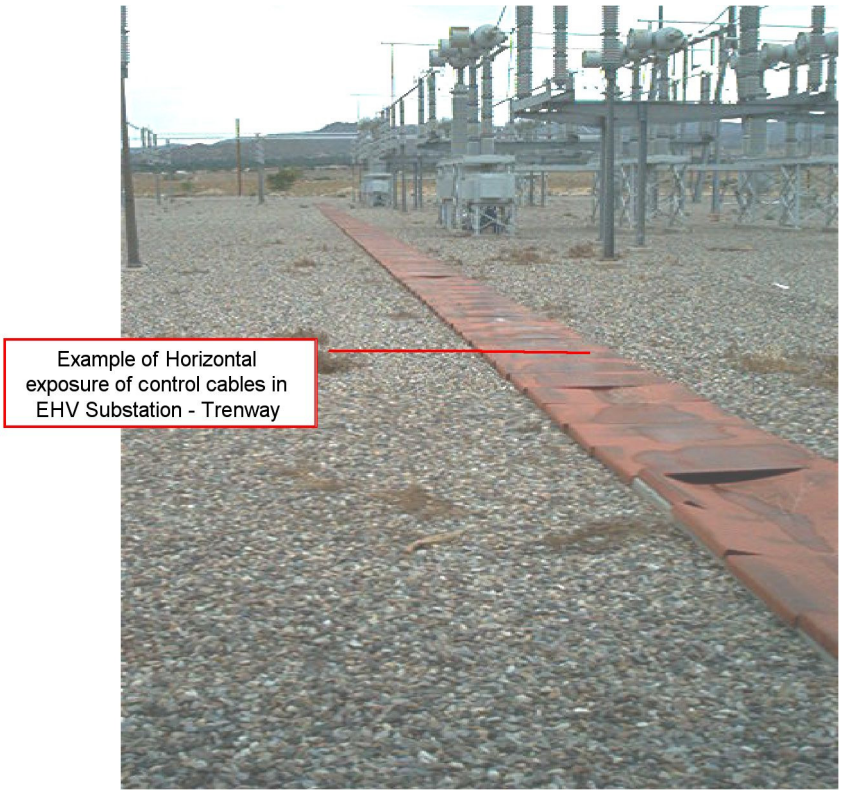

Figure 7-20. Second view of cable trenway.

In Figure 7-21 the cables are seen to be buried at a shallow depth. Under the cable insulation there is a metal external "shield", however the optical coverage of most of these braided shields is not usually very high, and generally does not provide significant shielding of the inner conductor at frequencies above 10 MHz.

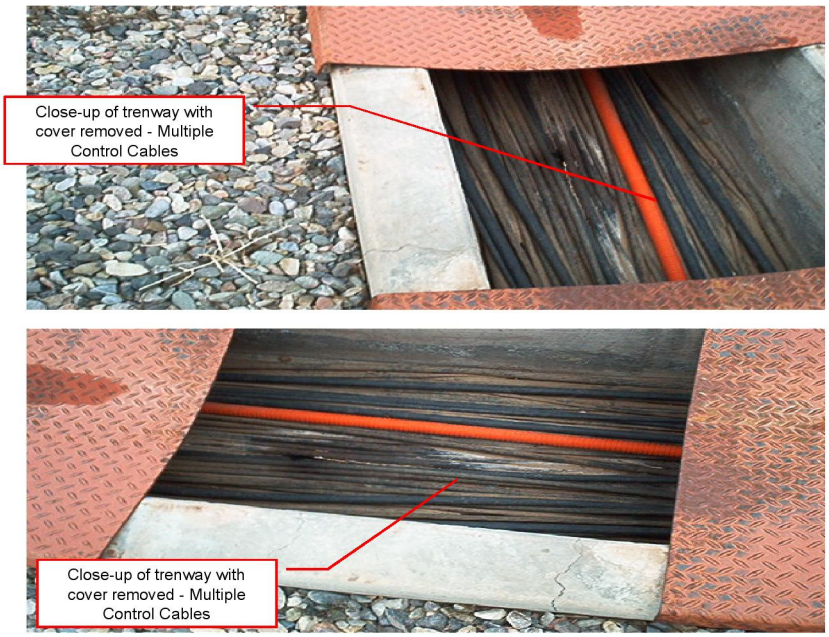

Figure 7-21. Control cables in trenway.

In Figure 7-22 the control cables have their insulation stripped back and the shields are connected to ground cables. It is noted that the ground cables are on the order of 30 cm long (or longer), which provides a high impedance at high frequencies. While this is sufficient for lightning frequencies (typically below 1 MHz), this will enable a significant portion of the high-frequency E1 HEMP transients to continue to propagate on the signal wires inside the control facility instead of being directed to ground.

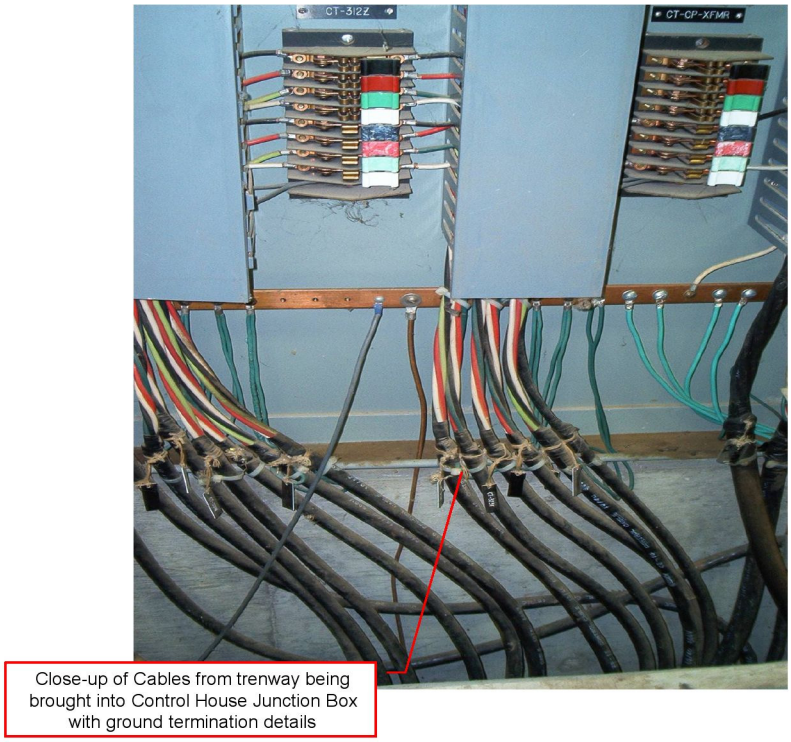

Figure 7-22. Grounding of control cable shields and j-boxes in control building.

In Figure 7-23 cables extend from the j-boxes to the individual racks of equipment. These cables will carry any remaining high-frequency transients that were coupled to the cables outside, and they will also be coupled to by the electromagnetic fields that propagate through the walls of the building. It is important to note that the direct coupling of fields inside the building is strongly influenced by the construction type of the building. There are strong variations for the penetrating electric fields at frequencies above 10 MHz due to whether the building is made of concrete (with or without reinforced bars), bolted metal, or wood.

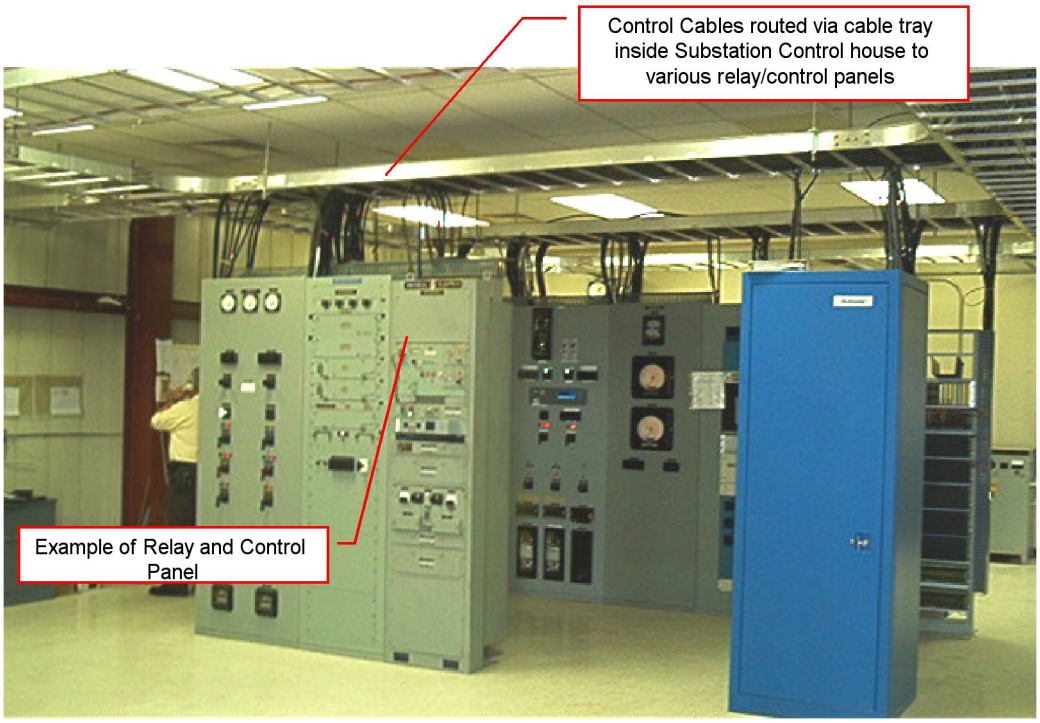

Figure 7-23. Distribution of control cables within building to cabinets.

While these figures are provided to give an indication of the scope of the problem, it will be necessary to evaluate many factors that are common or different in various power substations in order to determine the seriousness of the E1 HEMP threat and to recommend protection techniques that are cost effective.

Upon examination of Figures 7-4, 7-5 and 7-6, it appears that maximum levels of approximately 10 kV may be coupled to horizontal buried lines in a substation yard (top 1%). In Figure 7-7 levels of 70 kV may be induced on a vertical conduit. While the amount of these voltages that could propagate to the relays and other electronic control equipment is extremely variable, the fact that upsets on relays begin at 3.2 kV and damage to PLCs and PCs begin at approximately 0.5 kV, indicates a serious concern for the continued operation of a portion of the substations. When it is recognized that all of these substations shown in Figure 7-17 are exposed simultaneously (within one power cycle) it is clear that this threat is serious.

A second problem not discussed in detail indicates that even if the cable penetrations to the control building are protected, there is still the problem of the penetration of the E1 HEMP fields inside and coupling to the cables just above the electronic cabinets. The level of the field penetrating the building is completely dependent on the type of wall and ceiling construction; however, tests performed in the past on telephone switching centers indicated that voltage levels between 1 and 10 kV could be induced on cables. Depending on the way that the cables enter the cabinets (whether the shields are bonded or not) will determine if these voltages reach the electronic equipment ports inside.

7.4 Power Generation Facilities

Power generator facilities are similar to industrial processing plants in that they use PLCs to control the flow of fuel and other aspects of the power generation process. As indicated in Tables 7-5 and 7-6, damage may occur for E1-like pulses at levels as low as 0.6 kV, although only one manufacturer's equipment failed at that level. The other failed at 3.3 kV. Since power generators are manned, the impact of upset may not be as important as damage; however the damage levels indicated are quite low. In addition, it is not expected that the cabling within the generator facility will be better protected than in a substation, so again levels of induced voltages as high as 70 kV are likely to be coupled to vertical cables in a small portion of the generators.

7.5 Power Control Centers

Power control centers can be described as distributed computer facilities with many communications lines entering and leaving the facility. Since these facilities do not deal directly with high voltage transformers nearby, most of the computer equipment is not afforded the same basic level of immunity as those found in substations, or in power generation facilities for that matter. Equipment like the PC (see Table 7-8) will fail its communications port due to E1 HEMP at 0.5 kV, and other test data indicates that Ethernet ports are generally vulnerable at low levels. Given that ordinary building protection levels will typically allow 1 to 10 kV to be coupled to internal cables, this indicates a potential problem.

An important factor to consider is the location and type of wall construction of control centers. A control center built below the surface of the Earth has much better natural shielding than one built above grade in a high-rise building.

7.6 Distribution Line Insulators

Approximately 78% of all electric power delivery to end-users is delivered via 15 kV class distribution lines, as highlighted in Table 7-9. Figure 7-24 also illustrates a typical distribution feeder geometry that indicates the variation of the orientation of the lines for a single feeder. This shows that the likelihood for an optimum exposure of a segment of the line is high, and that at some point along the feeder the maximum E1 HEMP voltage will be induced, creating a possible insulator flashover.

Table 7-9. Summary of the distribution systems for the U.S. power grid.

U.S. Power Distribution

• Distribution systems in the U.S.
  ○ 5, 15, 25 and 35 kV
  ○ 15 kV is 77.5% of all load
  ○ 35,000 to 40,000 distribution substations
  ○ Substation size varies from ~1 - 100 MVA with an average of 20 MVA
 	
• Multiple feeders leave the substations
  ○ 4 to 14 feeders per substation
  ○ Typically 300 line segments per feeder
  ○ 60 fault protection and isolation devices per feeder
  ○ Average 3 phase feeder length is 10.8 miles
  ○ 93% of all U.S. feeders are of overhead construction
 	
• End users supplied by feeders
  ○ 13.0% industrial load
  ○ 18.4% supply urban/commercial load
  ○ 11.9% rural load
  ○ 55.7% suburban load

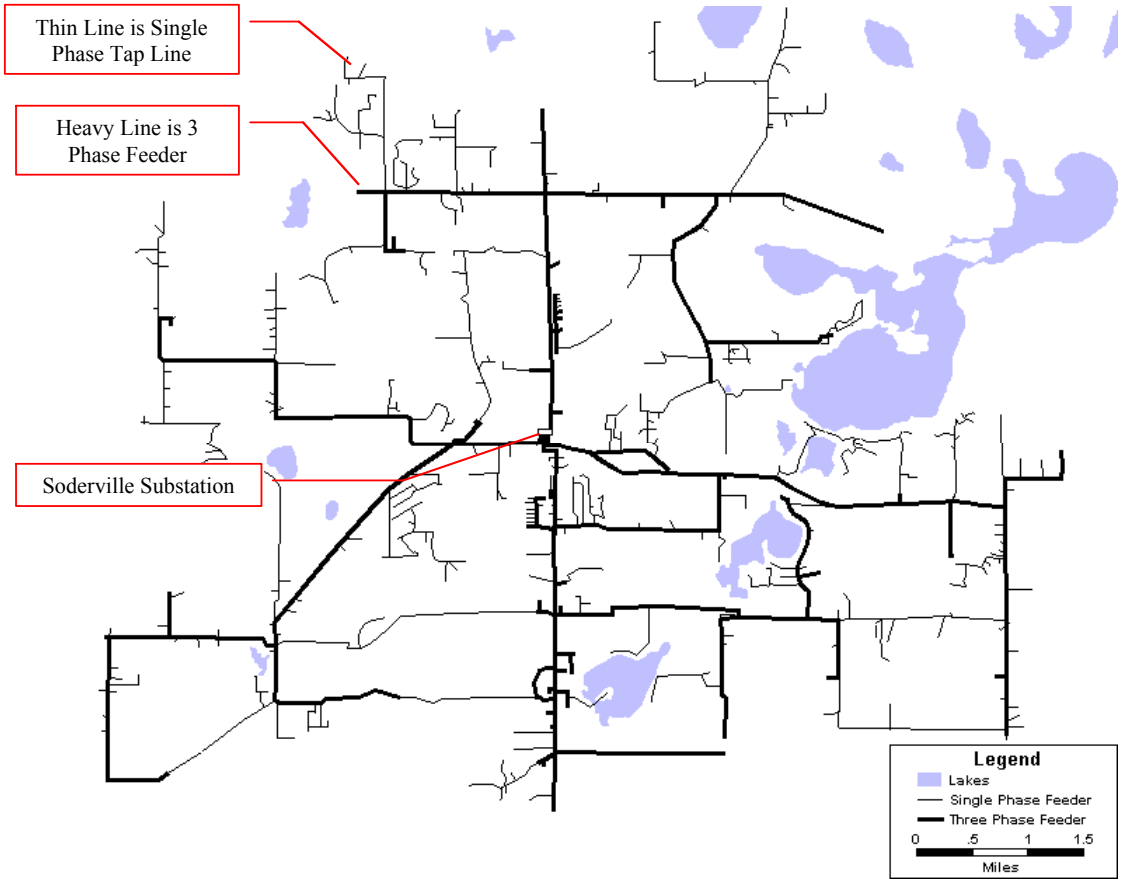

Figure 7-24. A typical above ground 15 kV distribution geometry in the U.S.

At present, considerable uncertainty exists as to whether the typical insulation capability of these distribution assets will be sufficient to withstand the induced overvoltages due to the E1 environment of a HEMP threat. Prior analysis of the E1 threat by Metatech indicated that induced overvoltages ranging from 200 kV to over 400 kV (depending on the scenario) can occur on these distribution lines over geographically widespread regions, and that if large scale distribution line insulator failure or flashover occurs, the impacted regions will likely experience power grid collapse.

Typical insulation design for distribution feeders usually are based upon the withstand (BIL, basic insulation level) of a 1.2 μs rise time impulse due to lightning (with a 50 μs pulse width). For these lightning impulses, typical pin insulator withstand generally starts at ~100 kV. It has generally been observed that the shorter duration pulse widths of the E1 HEMP threat will increase the level of the flashover voltage for these insulators, but the amount of increase was not well substantiated until further testing was performed.

Two sets of experiments and results are summarized here. The first is work done by Dr. Stan Gryzbowski from Mississippi State University (MSU), using standard insulator test techniques and testing of a wide variety of insulators found in the U.S. power grid. He also examined variations due to polarity of the impulse and other factors such as wet insulators. All of the testing was performed without power on the insulator, which is the usual method for testing insulators in the United States.

A second set of experiments and results are presented here for a set of Russian glass and porcelain insulators. The main emphasis for these experiments was the fact that the tests were performed both with no power on the insulators and also with the insulators energized with a portion of an AC waveform – up to 1,000 amperes.

7.6.1 Insulator Testing at MSU

A series of high voltage power lab tests were performed to establish the insulator performance for the steep front/short duration pulses environments typical from the E1 HEMP event. The High Voltage Laboratory at Mississippi State University (MSU) has had experience in generating pulses and conducting tests of insulators for these steep front/short duration pulses. The MSU lab can provide a test setup that will produce a ~50-60 ns pulse rise time while reaching pulse voltage peaks of as much as 900 kV. While the rise time is a bit slower than the expected E1 HEMP pulse rise time, the voltage peak levels and pulse width meet the test environment requirements fully. It is also believed that the pulse width of the E1 waveform is the critical parameter in understanding the peak voltage levels of flashover relative to the much wider lightning impulse tests.

The test plan of this project had the objective to determine the critical flashover (CFO) voltage, withstand voltage level and V-t characteristics for both major types of 15 kV insulators used in the U.S. – porcelain and polymer. (The CFO is the level with 50% probability of insulator arcing – and so possible disruption or damage to the power system.)

While porcelain insulators are the most common insulator type in use on the 15 kV U.S. distribution network, the application of polymer type insulators is more commonly used for new construction and/or for insulator replacements on existing distribution lines. The tested insulators are of pin type as well as suspension insulators. The evaluation of the CFO voltage and the V-t characteristics were conducted under dry and wet conditions for positive and negative polarity of the applied pulses.

Evaluation of the CFO voltage and V-t characteristics under steep front/short duration pulses (E1 type pulse) was performed on the following insulators (photo in Figure 7-25):

- porcelain pin type insulators: ANSI CLASS 55 - 4 and ANSI CLASS 55 – 3.
- porcelain suspension insulators: ANSI CLASS 52 - 1 and ANSI CLASS 52 – 9.
- 15 kV polymer suspension insulator, arcing distance 6.5 inch.

Figure 7-25. Insulators tested. This has two views of tested insulators, from the left: Pin type: ANSI 55-4, ANSI 55-3; Suspension type: ANSI 52-1, ANSI 52-9; 15 kV Polymer.

Test results are summarized in Tables 7-10, 7-11 and 7-12, showing both the peak CFO levels for the standard lightning tests, the steep front waveforms, and the ratio of those results. It is noted that in most cases the E1 HEMP related tests indicate that the peak HEMP voltage required is often less than a factor of 2 higher than the lightning BIL tests, and with negative polarity it is only about 10% higher. The polymer suspension insulator appears to be more robust to E1 HEMP waveforms. It is also recognized that apparently peak CFO voltages of much less than 200 kV are a concern for flashover.

Table 7-10. Insulator lightning results. This lists the peak CFO voltage, for both polarities, of the tested insulators under standard lightning impulse, in kV.

Configuration	Typical Application Line Voltage	POSITIVE POLARITY		NEGATIVE POLARITY	
		DRY	WET	DRY	WET
ANSI 55-4	13.2 kV	105	-	130	-
ANSI 55-3	11.5 kV	90	-	110	-
ANSI 52-1	13.2 kV	100	-	100	-
ANSI 52-9	13.2 kV	100	-	90	-
Polymer Suspension	<=15 kV	140	-	160	-

Table 7-11. Insulator fast pulse results. This gives the peak CFO voltage of the tested insulators under steep front, short duration pulses, in kV. Results are given for both pulse polarities, and wet and dry conditions.

Configuration	Typical Application Line Voltage	POSITIVE POLARITY		NEGATIVE POLARITY	
		DRY	WET	DRY	WET
ANSI 55-4	13.2 kV	282	201	135	133
ANSI 55-3	11.5 kV	153	160	117	127
ANSI 52-1	13.2 kV	119	131	132	141
ANSI 52-9	13.2 kV	126	132	122	130
Polymer Suspension	<=15 kV	358	299	308	371

Table 7-12. Effect of pulse type for insulator CFO voltage. This gives the ratio of peak CFO voltage at steep front, short duration pulse to the voltage for the lightning impulse.

Configuration	Typical Application Line Voltage	POSITIVE POLARITY		NEGATIVE POLARITY	
		DRY	WET	DRY	WET
ANSI 55-4	13.2 kV	2.7	-	1.04	-
ANSI 55-3	11.5 kV	1.7	-	1.06	-
ANSI 52-1	13.2 kV	1.2	-	1.32	-
ANSI 52-9	13.2 kV	1.3	-	1.36	-
Polymer Suspension	<=15 kV	2.6	-	1.93	-

7.6.2 Insulator Testing in Russia

Due to the fact that the Soviet Union indicated that some distribution insulators were damaged (resulting in power lines dropping to ground) during their high-altitude tests in 1962, they developed the capability to perform power-on tests on power line insulators. This testing is very difficult, but it was decided by the EMP Commission that such testing should be done and Metatech Corporation was the prime contractor for this test program.

The parameters used for the Russian testing included a fast pulser that could vary the rise time of the fast pulse between 20 and 40 ns with pulse widths of up to 100 ns. Peak voltages of slightly greater than 400 kV were also available. The tests included both porcelain and glass suspension insulators used on Russian 10 kV class power lines. Figure 7-26 is a photo of the glass insulator type tested. There was some examination of dry vs. wet vs. polluted insulator surfaces in the study, but the main interest was in the power-off vs. power-on test results.

Figure 7-26. Suspension glass insulator for 10 kV power line.

For the power-off tests, Table 7-13 illustrates the peak voltage for "overlap", which is the Russian term for flashover, for multiple tests on 4 different insulators. It is clearly observed that the variation in the flashover voltage is within measurement error. It is also interesting to see that there is not much variability between the 4 insulators tested.

Table 7-13. Peak levels of voltage for multiple tests (power off).

Insulator number	***Overlapping voltage, kV***			Notes
	First overlap	Second overlap	Third overlap	
1	360	380	370	-
2	380	400	400	-
3	400	370	390	-
4	390	380	400	-

Table 7-14 shows the variation of the characteristics of the insulators after flashover, as measured with "static" tests (these measurements look for insulator damage). There is also not much variation shown for insulator number 1 from Table 7-13.

Table 7-14. Characteristics of insulator number 1 after repeated flashovers (power off).

Measured parameter	Initial values	Value of parameter after overlapping		
		First overlap	Second overlap	Third overlap
Tangent of an angle of dielectric losses, %	2.9	2.8	3.2	2.9
Capacity, pF	56	55.5	57	56
Resistance, MOhm	7500	7400	7500	7400
Leakage current, μA	0.2	0.2	0.2	0.2

Comparable tests were then performed for the same types of insulators for a normal operational voltage of 14 kV and with a peak current of 1.8 kA available as follow current when an insulator flashed over. Several tests indicated that after a single flashover, the operating characteristics of nearly all of the insulators were degraded. In addition, it was found that the peak voltage level required for subsequent pulses were lower. Most dramatically, one of the six insulators tested was destroyed. Table 7-15 illustrates this behavior. Table 7-16 illustrates the degradation of the characteristics of insulator number 1, showing degradation in most of the measured parameters.

Table 7-15. Peak voltage of flashover for insulators under operational voltage.

Number of insulator	Voltage of overlapping, kV			Notes
	First overlap	Second overlap	Third overlap	
1	370	360	340	-
2	400	390	360	-
3	360	360	330	Destroyed after third test
4	370	320	280	-
5	380	360	330	-
6	390	380	340	-

Table 7-16. Characteristics of insulator number 1 after repeated flashovers (power on).

Measured parameter	Initial value	Values after overlapping		
		First overlap	Second overlap	Third overlap
Tangent of angle of dielectric losses, %	2.9	7.3	9.7	10.9
Capacity, pF	56.0	55.0	57.0	56.0
Resistance, Mohm	7500	6400	5500	3400
Leakage current, μA	0.2	0.4	0.5	0.7

For the case of insulator destruction, high-speed movies were taken in several cases. Figure 7-27 illustrates the fact that after the flashover occurs due to the fast voltage pulse, the power-follow provides the energy to destroy the insulator. Note that this did not happen in all cases, but it is likely that the mechanism for destruction has to do with small defects in the manufacture of the insulators. The Russian experimental team tried to determine whether these defects were present before the testing, but they were not able to find a simple way to evaluate this aspect.

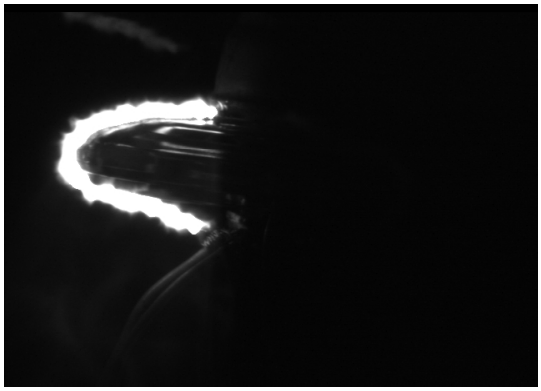

a. 0.5 ms

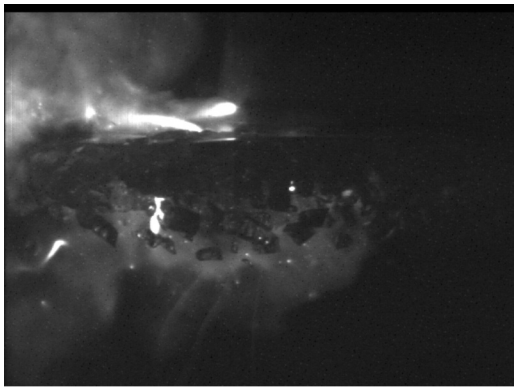

c. 10 ms

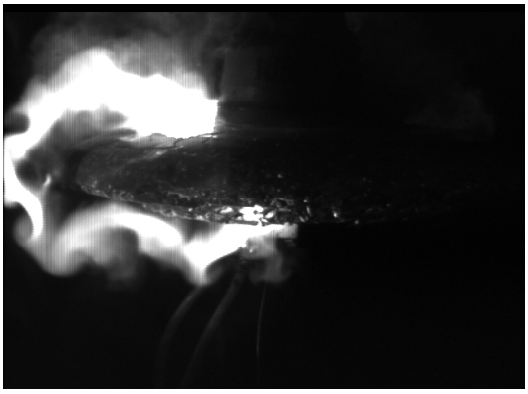

b. 2 ms

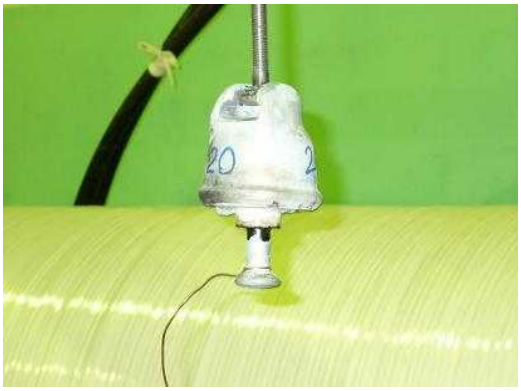

d. afterwards

Figure 7-27. Snapshots from an insulator test shot, with damage due to power follow. The frames are at times of 0.5 ms (a), 2 ms (b), and 10 ms (c); and after power is removed (d).

An important aspect of the multiple flashover testing under power is that while we do not expect large numbers of pulses to expose the U.S. power grid, lightning pulses are likely to occur in many locations in the U.S. and could therefore expose many insulators to previous impulses without causing noticeable failures. Thus a future E1 HEMP pulse could be the second or third pulse that some insulators will observe.

While this Russian test data is very dramatic, it is noted that the tests were performed on Russian insulators and statistical damage data were not obtained due to limitations in test time and funding. More work is needed to determine whether the damage aspect is a real concern in the U.S., and if so, with which types of insulator designs. It is clear however, that flashovers of U.S. insulators can occur at E1 HEMP voltage levels much lower than previously thought, and therefore some consideration of mitigation measures are needed, especially near the substations where the follow current will be high.

7.7 Distribution Transformers

During the ORNL power system studies in the 1980s, tests were performed to examine the possibility of E1 HEMP damage to distribution step-down transformers that can be found in the U.S. power grid. This testing included 19 samples of 7.2 kV/25 kVA power distribution transformers, using E1 HEMP like pulses. Damage that occurred was usually from dielectric breakdown within the windings – pinhole damage. The results of that testing are summarized in Table 7-17.

Table 7-17. 7.2 kV/25 kVA transformer failure testing for fast pulses.

XFMR	Shots #@kV	Peak Voltage (kV)	Time to Peak (ns)	Surge Arrester	Notes	Result
ZS1						Pulser calibration
ZS2	1@400	264	618	No	(1)	T-T failure
ZS3	2@400	288	668	No	(2)	HV-LV failure
ZS4	2@400	280	600	No	(1)	L-L failure
ZS5	1@400	272	550	No	(2)	HV-LV failure
ZS6	2@400	290	643	No	(1)	No damage
ZV1	1@400	296	601	No	(1)	No damage
ZV2	1@400	304	592	No	(2)	HV-LV failure
ZV3	2@400	110	100	Yes	(3)	No damage
ZV4	2@500	110	100	Yes	(3)	No damage
ZV4	2@780	116	110	Yes	(3)	No damage
XV1	1@400	272	500	No	(2)	HV-LV failure
XV2	2@400	115	110	Yes	(3)	No damage
ZW1	2@400	292	552	No	(1)	No damage
ZW2	2@400	16	Oscillatory	No	(4)	No damage
ZW3	2@780	100	110	Yes	(3)	No damage
ZW4	2@1000	112	105	Yes	(3)	No damage
ZD1	2@400	120	550	No	(5)	No damage
ZD2	2@400	20	Oscillatory	No	(4)	No damage
ZE1	2@1000	95	100	Yes	(6)	No damage
ZE2	6@780	95	100	Yes	(6)	No damage

(1) External flashover on HV bushing: T-T failure denotes turn-to-turn failure; L-L failure denotes line-to-line failure
(2) No external flashover; HV-LV failure denotes a high-voltage winding flashover to the low-voltage winding
(3) Surge arrester operation and no external flashover
(4) Surge applied to the low-voltage bushings with no external flashover
(5) Surge applied common mode to both HV bushings with external flashover
(6) Surge applied common mode to both bushings, and both arresters operated

It is noted in the test results that failures occurred when the peak fast pulse voltage was between 264 and 304 kV. No damage occurred for peak pulses of 290 and 296 kV, so there appears to be some variability within the group of 19 transformers, although the variation is not that great. When lightning surge arresters were added to the transformers, no damage was noted up to the capability of the pulser (which was 1000 kV). The conclusion reached by the test team, however, indicated that standard surge arresters mounting procedures often include a long wire lead to the transformer, and this method of mounting might not allow for the lightning surge arrester to protect the transformer from fast pulses. Also, not all areas of the U.S. use lightning protection on distribution transformers (e.g. coastal California).

Section 8
Impacts on Society of E1 HEMP Power System Failures

The EMP Commission specifically was tasked to look at the impacts on general society from an EMP assault on the U.S. It noted that this is not just a power system issue – all of the other important legs of the infrastructure are also intertwined with each other and the power system, with the power grid probably being the most significant. Note also that E1 HEMP often cannot be isolated from other effects. E2 and E3 are also important, and possibly would have worse effects than E1 for some parts of the infrastructure, such as the effect of E3 on the power transmission system. Also there can be synergistic effects, such as E1 setting up a system to be further damaged by the following E2 or E3 pulse. And there are also other possible similar EM threats to the infrastructures, such as geomagnetic storms (with similarities to E3) and IEMI (intentional electromagnetic interference). IEMI has similarities to E1 HEMP in regard to the vulnerability of control, sensor, and communication lines. However, IEMI is unlikely to be a threat for power distribution insulators and transformers – for the simple fact that the high height and the inability to provide a plane wave source over 100 meters means that IEMI emitters will not be effective in coupling large voltages to long power lines.

Several issues were evaluated by the EMP commission:

1. Electronic controls are being used more and more in all aspects of our lives. This is especially true of any large-scale processing system, such as in all types of factories, but also in many aspects of our infrastructures. Certainty this is true for any unmanned station. There are controllers (such as PLCs), communication devices, and sensors. Power substations and pipelines make extensive use of these devices, which are susceptible to E1 HEMP effects.
2. EM assaults can interfere with control systems. This has been shown to be true by many experiences, and is why EMC/EMI (electromagnetic compatibility, electromagnetic interference) is so important in our modern world. For example, on July 29, 1967, an armed missile was launched from a fighter aircraft on the deck of the aircraft carrier Forrestal, causing extensive damage and killing 134 sailors. This was thought to be due to two problems, a malfunction of a connector on the missile system and a failure of a safety device, with a radar signal being the trigger of the mishap. Another problem, described in Figure 8-1, is a breakdown in the control of a water pipeline in San Diego, which was due to interference from a radar 25 miles offshore.
3. Outages have occurred in the past – large ones infrequently. Geomagnetic storms have caused some (and so, similarly, E3 is a threat to the grid). It might not be perfectly clear what caused some of the others, but none are believed to be caused by effects similar to E1 HEMP. But confusion and lack of good data of the state of all aspects of the vast power system has contributed to outage growth (the August 14, 2003 outage). With E1 HEMP simultaneously hitting a large area, distorting and interrupting communications, and damaging devices in the SCADA system, similar, or worse, could be expected.
4. The EMP Commission emphasized the interdependence of the various legs of the infrastructures. So much of modern society depends on the electric power system,

and often there is, at best, very limited back-up power. The issues include the need for communication to try to minimize the spread of an outage, and the need for many aspects of the infrastructure to recover from outages. In all, communications is an important issue, possibly secondary to the power system itself. There are also pipelines that transport fuels, such as natural gas and oil that might be needed to run a power station. Also, getting repair people out to fix HEMP damage involves communication, and fueling vehicles, while gas stations often shut down when electric power is out.

In November 1999, San Diego County Water Authority and San Diego Gas and Electric companies experienced severe electromagnetic interference to their SCADA wireless networks. Both companies found themselves unable to actuate critical valve openings and closings under remote control of the SCADA electronic systems. This inability necessitated sending technicians to remote locations to manually open and close water and gas valves, averting, in the words of a subsequent letter of complaint by the San Diego County Water Authority to the Federal Communications Commission, a potential "catastrophic failure" of the aqueduct system. The potential consequences of a failure of this 825 million gallon per day flow rate system ranged from "spilling vents at thousands of gallons per minute to aqueduct rupture with ensuing disruption of service, severe flooding, and related damage to private and public property." The source of the SCADA failure was later determined to be radar operated on a ship 25 miles off the coast of San Diego.

Figure 8-1. An example of the failure of an infrastructure system due to EM assault.

It should be noted that besides determining what damage might happen, it is also important to evaluate the recovery process. How long would it take to do the repairs, especially when so many other parts of the infrastructures might also be out of service? For E1 HEMP effects, most of the damage would be to smaller type devices – such as those that fail randomly now and then. Technicians will need to search to find what is damaged, and replace or repair it. Of course, this could be a formidable task if there is much damage over a large region. An E1 HEMP attack is unlikely to cause damage to very large transformers, such as is suspected that E3 could do – damage that could take years to repair. Probably the only way E1 HEMP would cause that level of long term massive damage would be if confusion of controls triggered the power system to destroy itself, which is certainly possible, but very unpredictable.

As a final note, the bottom line for predicting E1 HEMP effects is that our modern world has never experienced such as assault. We can try to predict effects and draw upon similar effects and experimentation, but there is always the possibility of some surprise. Often even somewhat minor issues have lead to extensive problems in the past, which would not have been predicted. It is also not known how American society in general would react if massive infrastructure failures occur over a large region and for a long time.

Section 9
Bibliography of E1 HEMP References

9.1 General E1 HEMP References

Air Force Weapons Laboratory, "EMP Interaction: Principles, Techniques, and Reference Data", AFWL-TR-80-402 (EMP Interaction 2-1), Dikewood Industries, Inc., December 1980.

Baum, C.E., "Electron Thermalization and Mobility in Air", Theoretical Note 12, July 1965.

Bridgeman, Charles J., *Introduction to the Physics of Nuclear Weapons Effects*, Defense Threat Reduction Agency, July 2001 (limited distribution).

Burke, P., and H. Fowles, "Pulsed Current Injection Testing with Short Duration (E1-Like) Pulses", MRC/ABQ-R-1315, Mission Research Corporation, Volumes I and II, May 1990.

Butler, C., et al., "EMP Penetration Handbook for Apertures, Cable Shields, Connectors, Skin Panels", AFWL-TR-77-149, Air Force Weapons Laboratory (The Dikewood Corporation), December 1977.

Davies, D., and P. Chantry, "Air Chemistry Measurements I", DC-TN-2030.301-1, Dikewood Division of Kaman Sciences Corporation, November 1982.

Defense Threat Reduction Agency, "EM-1, Capabilities of Nuclear Weapons" (unpublished).

Defense Threat Reduction Agency, "Reaction Rate Handbook", DNA 1948H, March 1972.

DoD-STD-2169A, "Military Standard - High Altitude Electromagnetic Pulse (HEMP) Environment", December 1987 (unpublished).

General Electric Company – TEMPO, "DNA EMP (Electromagnetic Pulse) Handbook", July 1979 (downgraded, limited distribution).
"Volume 1 – Design Principles", DNA 2114H-1,
"Volume 2 – Coupling Analysis", DNA 2114H-2,
"Volume 3 – Component Response and Test Methods", DNA 2114H-3,
"Volume 4 – Environment and Applications", DNA 2114H-4,
"Volume 5 – Resources", DNA 2114H-5,
"Volume 6 – Computer Codes", DNA 2114H-6.

Ghose, Rabindra N., *EMP Environment and System Hardness Design*, Don White Consultants, Inc., 1984.

Glasstone, Samuel, and Philip J. Dolan, *The Effects of Nuclear Weapons*, U.S. Departments of Defense and Energy, 1977 (1st edition: 57, 2nd edition 1962).

Grzybowski, Dr. S., and Yang Song, “Investigation on the Electrical Strength of the Distribution Line Elements Under Steep Front, Short Duration Pulses”, Mississippi State University, January 2004.

Karzas, W.J., and R. Latter, "Electromagnetic Radiation from a Nuclear Explosion in Space”, *Physical Review,* Vol. 126, June 1962.

Karzas, W.J., and R. Latter, "The Electromagnetic Signal Due to the Interactions of Nuclear Explosions with the Earth's Magnetic Field”, *Journal of Geophysical Research,* Vol. 67, November 1962.

Karzas, W.J., and R. Latter, “EMP from High-Altitude Nuclear Explosions”, Report No. RM-4194, Rand Corporation, March 1965 (unpublished).

Karzas, W.J., and R. Latter, "Detection of Electromagnetic Radiation from Nuclear Explosions in Space”, *Physical Review,* Vol. 137, March 1965.

Kompaneets, A.S., "Radio Emission From an Atomic Explosion”, *Soviet Physics JETP,* December 1958.

Longmire, C.L., "On the Electromagnetic Pulse Produced by Nuclear Explosions", *IEEE Trans. Ant. & Prop.,* Vol. AP-26, No. 1, January 1978.

Longmire, C.L., "Introduction to EMP Generation Theory", *Journal of Defense Research,* Special Issue 84-1, May 1985, pp. 91-95 (unpublished).

Longmire, C.L., and J. Koppel, “Formative Time Lag of Secondary Ionization”, MRC-R-88, Mission Research Corporation, January 1974.

Messenger, G. C. and M. S. Ash, *The Effects of Radiation on Electronic Systems*, Van Nostrand Reinhold Company, 1986.

Miller, D.B., “Experimental Investigation of Steep-Front Short Duration (SFSD) Surge Effects on Power System Components”, ORNL/Sub/87-92345, Oak Ridge National Laboratory, May 1992.

MIL-HDBK-423, “High-Altitude Electromagnetic Pulse (HEMP) Protection for Fixed and Transportable Ground-Based Facilities, Volume I Fixed Facilities”, 15 May 1993.

MIL-STD-188-125-1, “Department of Defense Interface Standard. High-Altitude Electromagnetic Pulse (HEMP) Protection for Ground-Based C4I Facilities Performing Critical, Time-Urgent Missions, Part 1 Fixed Facilities”, 17 July 1998.

Northrop, John, *Handbook of Nuclear Weapon Effects, Calculational Tools Abstracted from DSWA’s Effects Manual One (EM-1)*, Defense Threat Reduction Agency, September, 1996 (limited distribution).

Parfenov, Y., “Research of Physical Laws of the Flashover and Damage of Power Line Insulators due to Fast Voltage Pulses with Power On and Power Off is Important Problem”, Institute for High Energy Densities, January 25, 2004.

Radasky, W. A. and R. L. Knight, HAPS — A Two Dimensional High Altitude EMP Environment Code, Air Force Weapons Laboratory, EMP TN 125, November 1971.

Radasky, W. A., W. J. Karzas, G. K. Schlegel and C. W. Jones, High Altitude Electromagnetic Pulse — Theory and Calculations, Defense Nuclear Agency, DNA TR 88 123, 3 October 1988.

Radasky, W. A., "High-altitude EMP (HEMP) Environments and Effects," NBC Report, Spring/Summer 2002, pp. 24-29.

Radasky, W. A., "High-Altitude Electromagnetic Pulse (HEMP): A Threat to Our Way of Life," IEEE USA Today's Engineer, September 2007.

Radasky, W., "Approach for Protection of HV Power Grid Network Control Electronics from Intentional Electromagnetic Interference (IEMI)", CIGRE SC C4 2009 Kushiro Colloquium, June 2009.

Rickets, L. W., *Fundamentals of Nuclear Hardening of Electronic Equipment*, Wiley & Sons, Inc., 1972.

Rickets, L. W., J. E. Bridges, and J. Miletta, *EMP Radiation and Protective Techniques*, Wiley & Sons, Inc., 1976.

Rudie, Norman J., *Principles and Techniques of Radiation Hardening*, 2nd ed., 1976:
"Volume 1: Interaction of Radiation with Matter and Material Effects",
"Volume 2: Transient Radiation Effects in Electronics (TREE)",
"Volume 3: Electromagnetic Pulse (EMP) and System Generated EMP".

Sandia Laboratories, "Electromagnetic Pulse Handbook for Missiles and Aircraft in Flight", SC-M-71 0346, AFWL TR 73-68, EMP Interaction Note 1-1, September, 1972.

Schaefer, R.R., "Defense Special Weapons Agency ELECTRA Program Technical Review Group Test Objects 1, 2, and 3", LRDA-TR-211-7221-3001-001, Logicon R&D Associates, January 1997 (unpublished).

Schaefer, R.R., F.C. Dumont, and C.R. Grain, "High-Altitude Electromagnetic Pulse (HEMP) Hardness Maintenance/Hardness Surveillance for Fixed, Ground-Based C4I Facilities, Volumes 1-3", DNA-TR-93-186-V1 through V3, April 1995.

Schlegel, G.K., M.A. Messier, W.A. Radasky, and W.C. Hart, "EMP Environment Handbook", AFWL EMP Phenomenology 1-1, January 1972 (unpublished).

Sherman, R., et al., *EMP Engineering and Design Principles*, Bell Telephone Laboratories Report, 1975.

9.2 IEC HEMP References

IEC, "Electromagnetic compatibility (EMC) - Part 1-3: General - The effects of high-altitude EMP (HEMP) on civil equipment and systems", IEC 61000-1-3, International Electrotechnical Commission, Geneva, Switzerland

IEC, “Electromagnetic compatibility (EMC) - Part 1-5: General - High power electromagnetic (HPEM) effects on civil systems”, IEC 61000-1-5, International Electrotechnical Commission, Geneva, Switzerland

IEC, “Electromagnetic compatibility (EMC) - Part 2: Environment - Section 3: Description of the environment - Radiated and non-network-frequency-related conducted phenomena”, IEC 61000-2-3, International Electrotechnical Commission, Geneva, Switzerland

IEC, “Electromagnetic compatibility (EMC) - Part 2: Environment - Section 5: Classification of electromagnetic environments. Basic EMC publication”, IEC 61000-2-5, International Electrotechnical Commission, Geneva, Switzerland

IEC, “Electromagnetic compatibility (EMC) - Part 2: Environment - Section 9: Description of HEMP environment - Radiated disturbance. Basic EMC publication”, IEC 61000-2-9, International Electrotechnical Commission, Geneva, Switzerland

IEC, “Electromagnetic compatibility (EMC) - Part 2-10: Environment - Description of HEMP environment - Conducted disturbance”, IEC 61000-2-10, International Electrotechnical Commission, Geneva, Switzerland

IEC, “Electromagnetic compatibility (EMC) - Part 2-11: Environment - Classification of HEMP environments”, IEC 61000-2-11, International Electrotechnical Commission, Geneva, Switzerland

IEC, “Electromagnetic compatibility (EMC) - Part 2-13: Environment - High-power electromagnetic (HPEM) environments - Radiated and conducted”, IEC 61000-2-13, International Electrotechnical Commission, Geneva, Switzerland

IEC, “Electromagnetic compatibility (EMC) - Part 4-1: Testing and measurement techniques - Overview of IEC 61000-4 series”, IEC 61000-4-1, International Electrotechnical Commission, Geneva, Switzerland

IEC, “Electromagnetic compatibility (EMC)- Part 4-2: Testing and measurement techniques - Electrostatic discharge immunity test”, IEC 61000-4-2, International Electrotechnical Commission, Geneva, Switzerland

IEC, “Electromagnetic compatibility (EMC) - Part 4-3 : Testing and measurement techniques - Radiated, radio-frequency, electromagnetic field immunity test”, IEC 61000-4-3, International Electrotechnical Commission, Geneva, Switzerland

IEC, “Electromagnetic compatibility (EMC) - Part 4-4: Testing and measurement techniques - Electrical fast transient/burst immunity test”, IEC 61000-4-4, International Electrotechnical Commission, Geneva, Switzerland

IEC, “Electromagnetic compatibility (EMC) - Part 4-5: Testing and measurement techniques - Surge immunity test”, IEC 61000-4-5, International Electrotechnical Commission, Geneva, Switzerland

IEC, “Electromagnetic compatibility (EMC) - Part 4-6: Testing and measurement techniques - Immunity to conducted disturbances, induced by radio-frequency fields”, IEC 61000-4-6, International Electrotechnical Commission, Geneva, Switzerland

IEC, “Electromagnetic compatibility (EMC) - Part 4-12: Testing and measurement techniques - Ring wave immunity test”, IEC 61000-4-12, International Electrotechnical Commission, Geneva, Switzerland

IEC, “Electromagnetic compatibility (EMC) - Part 4-18: Testing and measurement techniques - Damped oscillatory wave immunity test”, IEC 61000-4-18, International Electrotechnical Commission, Geneva, Switzerland

IEC, “Electromagnetic compatibility (EMC) - Part 4-20: Testing and measurement techniques - Emission and immunity testing in transverse electromagnetic (TEM) waveguides”, IEC 61000-4-20, International Electrotechnical Commission, Geneva, Switzerland

IEC, “Electromagnetic compatibility (EMC) - Part 4-21: Testing and measurement techniques - Reverberation chamber test methods”, IEC 61000-4-21, International Electrotechnical Commission, Geneva, Switzerland

IEC, “Electromagnetic compatibility (EMC) - Part 4-23: Testing and measurement techniques - Test methods for protective devices for HEMP and other radiated disturbances”, IEC 61000-4-23, International Electrotechnical Commission, Geneva, Switzerland

IEC, “Electromagnetic compatibility (EMC) - Part 4-24: Testing and measurement techniques - Section 24: Test methods for protective devices for HEMP conducted disturbance - Basic EMC Publication”, IEC 61000-4-24, International Electrotechnical Commission, Geneva, Switzerland

IEC, “Electromagnetic compatibility (EMC) - Part 4-25: Testing and measurement techniques - HEMP immunity test methods for equipment and systems”, IEC 61000-4-25, International Electrotechnical Commission, Geneva, Switzerland

IEC, “Electromagnetic compatibility (EMC) - Part 4-32: Testing and measurement techniques - High-altitude electromagnetic pulse (HEMP) simulator compendium”, IEC 61000-4-32, International Electrotechnical Commission, Geneva, Switzerland

IEC, “Electromagnetic compatibility (EMC) - Part 4-33: Testing and measurement techniques - Measurement methods for high-power transient parameters”, IEC 61000-4-33, International Electrotechnical Commission, Geneva, Switzerland

IEC, “Electromagnetic compatibility (EMC) - Part 4-35: Testing and measurement techniques - HPEM simulator compendium”, IEC 61000-4-35, International Electrotechnical Commission, Geneva, Switzerland

IEC, “Electromagnetic compatibility (EMC) - Part 5: Installation and mitigation guidelines - Section 1: General considerations - Basic EMC publication”, IEC 61000-5-1, International Electrotechnical Commission, Geneva, Switzerland

IEC, “Electromagnetic compatibility (EMC) - Part 5: Installation and mitigation guidelines - Section 2: Earthing and cabling”, IEC 61000-5-2, International Electrotechnical Commission, Geneva, Switzerland

IEC, “Electromagnetic compatibility (EMC) - Part 5-3: Installation and mitigation guidelines - HEMP protection concepts”, IEC 61000-5-3, International Electrotechnical Commission, Geneva, Switzerland

IEC, “Electromagnetic compatibility (EMC) - Part 5: Installation and mitigation guidelines - Section 4: Immunity to HEMP - Specifications for protective devices against HEMP radiated disturbance. Basic EMC Publication”, IEC 61000-5-4, International Electrotechnical Commission, Geneva, Switzerland

IEC, “Electromagnetic compatibility (EMC) - Part 5: Installation and mitigation guidelines - Section 5: Specification of protective devices for HEMP conducted disturbance. Basic EMC Publication”, IEC 61000-5-5, International Electrotechnical Commission, Geneva, Switzerland

IEC, “Electromagnetic compatibility (EMC) - Part 5-6: Installation and mitigation guidelines - Mitigation of external EM influences”, IEC 61000-5-6, International Electrotechnical Commission, Geneva, Switzerland

IEC, “Electromagnetic compatibility (EMC) - Part 5-7: Installation and mitigation guidelines - Degrees of protection provided by enclosures against electromagnetic disturbances (EM code)”, IEC 61000-5-7, International Electrotechnical Commission, Geneva, Switzerland

IEC, “Electromagnetic compatibility (EMC) - Part 5-8: Installation and mitigation guidelines - HEMP protection methods for the distributed infrastructure”, IEC 61000-5-8, International Electrotechnical Commission, Geneva, Switzerland

IEC, “Electromagnetic compatibility (EMC) - Part 5-9: Installation and mitigation guidelines - System-level susceptibility assessments for HEMP and HPEM”, IEC 61000-5-9, International Electrotechnical Commission, Geneva, Switzerland

IEC, “Electromagnetic compatibility (EMC) - Part 6-1: Generic standards - Immunity for residential, commercial and light-industrial environments”, IEC 61000-6-1, International Electrotechnical Commission, Geneva, Switzerland

IEC, “Electromagnetic compatibility (EMC) - Part 6-2: Generic standards - Immunity for industrial environments”, IEC 61000-6-2, International Electrotechnical Commission, Geneva, Switzerland

IEC, “Electromagnetic compatibility (EMC) - Part 6-5: Generic standards - Immunity for power station and substation environments”, IEC 61000-6-5, International Electrotechnical Commission, Geneva, Switzerland

IEC, “Electromagnetic compatibility (EMC) - Part 6-6: Generic standards - HEMP immunity for indoor equipment”, IEC 61000-6-6, International Electrotechnical Commission, Geneva, Switzerland

9.3 EMP Commission and Related References

Dr. John S. Foster, Jr., et al., "Report of the Commission to Assess the Threat to the United States from Electromagnetic Pulse (EMP) Attack, Volume 1: Executive Report", 2004.

Dr. John S. Foster, Jr., et al., "Report of the Commission to Assess the Threat to the United States from Electromagnetic Pulse (EMP) Attack, Critical National Infrastructures", April 2008.

J.G. Kappenman, W.A. Radasky and J.L. Gilbert, "Evaluation of the Vulnerability of the NGC Power Transmission Grid to the Effects of Geomagnetic Storms", May 8, 1998, Meta-R-144.

J.G. Kappenman, "Evaluation of the Vulnerability of the CEPCO Transmission Network to the Effects of Geomagnetic Storms", March 2001, Meta-R-182.

J.G. Kappenman, J.J. Patrick, J.L. Gilbert, E.B. Savage and W. A. Radasky, "An Expedited Geomagnetic Storm and Late-Time HEMP Threat Analysis Study to Assess the Vulnerability of the U.S. Power Grid", Prepared for the EMP Commission, December 31, 2002, Meta-R-208.

W.A. Radasky, J.L. Gilbert, E.B. Savage, J.G. Kappenman, J.J. Patrick, M.A. Messier and P.R. Barnes, "An Expedited early-Time HEMP Threat Analysis Study to Assess the Vulnerability of the U.S. Power Grid", Prepared for the EMP Commission, December 31, 2002, Meta-R-209.

W.A. Radasky, J.L. Gilbert and E.B. Savage, "The Use of the Russian HEMP E3 Measurements for Model Verification", Meta-R-218.

J.G. Kappenman, J.J. Patrick, J.L. Gilbert, W.A. Radasky and E.B. Savage, "Power Grid Restoration Report: Analysis of Power Grid Restoration Concerns Due to Large E3-Initiated Power Grid Collapses", Prepared for the EMP Commission, November 2003, Meta-R-222.

E.B. Savage, W.A. Radasky, J.G. Kappenman, J.L. Gilbert, K.S. Smith and M.J. Madrid, "HEMP Impulse Injection Testing of Power System Electronics and Electrical Components", Prepared for the EMP Commission, December 29, 2003, Meta-R-225.

W.A. Radasky, J.G. Kappenman, E.B. Savage and J.L. Gilbert, "Metatech Recommendations to the EMP Commission", Prepared for the EMP Commission, December 31, 2003, Meta-R-226.

Gilbert J.L, W.A. Radasky, J.G. Kappenman, E.B. Savage, K.S. Smith and M.J. Madrid, "Final Report of Scenario Results Volume 2: E1 HEMP Effects", Prepared for the EMP Commission, January 16, 2004, Meta-R-227.

J.G. Kappenman, J.J. Patrick, J.L. Gilbert, E.B. Savage and W.A. Radasky, "Initial Report on Outage and Restoration Concerns for the U.S. Power Grid Due to HEMP Threats", Prepared for the EMP Commission, June 1, 2003, Meta-R-229.

J.G. Kappenman, J.J. Patrick, J.L. Gilbert, E.B. Savage and W.A. Radasky, "Interim Report on Outage and Restoration Concerns for the U.S. Power Grid Due to Late-Time HEMP Threats (Deliverable 2)", Prepared for the EMP Commission, July 15, 2003, Meta-R-230.

J.G. Kappenman, J.J. Patrick, W.A. Radasky and E.B. Savage, "Detailed Test Plan Including Ordered Equipment" Prepared for the EMP Commission, September 18, 2003, Meta-R-231.

J.G. Kappenman, J.J. Patrick, J.L. Gilbert, E.B. Savage and W.A. Radasky, "Final Outage and Restoration Results (Deliverable 3) An Overview of Major International Power System Blackouts and System Restorations", Prepared for the EMP Commission, September 8, 2003, Meta-R-232.

W.A. Radasky, "Russian Research Activities Work Plan for Research", Prepared for the EMP Commission, October 3, 2003, Meta-R-233.

E.B. Savage, J.L. Gilbert, K.S. Smith, M.J. Madrid and W.A. Radasky, "Preliminary Test Results: Fast Pulse Testing of Allen Bradley MicroLogix 1000 PLC (Programmable Logic Controller)", Prepared for the EMP Commission, October 30, 2003, Meta-R-234.

W.A. Radasky, "Russian Research Activities Preliminary Results", Prepared for the EMP Commission, January 16, 2004, Meta-R-235.

W.A. Radasky, "Russian Research Activities Summary of Washington, DC Meeting Held on 9 December 2003 at IDA", Prepared for the EMP Commission, Meta-R-236.

J.G. Kappenman, J.J. Patrick, W.A. Radasky, E.B. Savage, J.L. Gilbert, K.S. Smith and M.J. Madrid "Draft Research Report: Metatech Work for the EMP Commission", Prepared for the EMP Commission, January 30, 2004, Meta-R-237.

W.A. Radasky, J.G. Kappenman and P. Warner "Report on Evaluation of Harmonics Data from SARA Field Tests" October 1, 2006, Meta-R-271.

W.A. Radasky, "The Threat of High-Altitude Electromagnetic Pulse (HEMP) on the U.S. Power Infrastructure (Deliverable 4.2.1a) December 18, 2006, Meta-R-274.

W.A. Radasky and J.G. Kappenman, "The Threat of a 100 Year Geomagnetic Superstorm to the U.S. Power Infrastructure" 25 January 2007, Meta-R-280R2.

J.G. Kappenman, P. Warner and W.A. Radasky. "TEST REPORT: Report on Evaluation of UPS Performance, Complex Load Recommendations and Harmonic Propagation and Modeling Analysis to Support Additional SARA Field Tests" Meta-R-282, 26 March 2007, Meta-R-282.

J.G. Kappenman, P. Warner and W.A. Radasky. " TEST REPORT: Report on Task 2a Modeling Analysis to Support Additional SARA Field Tests", May 11, 2007, Meta-R-284.

F.M. Tesche, "HEMP Field Penetration into Poorly Shielded Enclosures and Coupling to Internal Conductors", June 4, 2007, Meta-R-287.

W.A. Radasky, “The Threat of Non-Nuclear EMP on the U.S. Infrastructure (Deliverable 4.3)” September 30, 2007, Meta-R-294.

J.G. Kappenman, “An Assessment of the Threat Potential to the U.S. Electric Power Grids from Extreme Space Weather Storms – Analysis of U.S. Power System Impacts from Large Geomagnetic Storm Events (Task A-C)” October 1, 2007, Meta-R-295.

J.G. Kappenman and P. Warner, “An Assessment of the Threat Potential to the U.S. Electric Power Grids from Extreme Space Weather Storms – Analysis of U.S. Power System Impacts from Large Geomagnetic Storm Events (Deliverable 4.6 – Part 1 of 3)” October 24, 2007, Meta-R-297.

J.G. Kappenman and P. Warner, “An Assessment of the Threat Potential to the U.S. Electric Power Grids from Extreme Space Weather Storms – Analysis of U.S. Power System Impacts from Large Geomagnetic Storm Events (Deliverable 4.6 – Part 2 of 3)” October 24, 2007, Meta-R-298.

J.G. Kappenman and P. Warner, “An Assessment of the Threat Potential to the U.S. Electric Power Grids from Extreme Space Weather Storms – Analysis of U.S. Power System Impacts from Large Geomagnetic Storm Events–U.S. West (Deliverable 4.6 – Part 3 of 3)” November 19, 2007, Meta-R-299.

J.G. Kappenman, P. Warner and W.A. Radasky. “Analysis of U.S. Power Grid Hardening Options Due to E3 HEMP” November 14, 2008, Meta-R-307.

W.A. Radasky, J.G. Kappenman, J.L. Gilbert and E.B. Savage, “Recommendations for the Protection of the Oahu High Voltage Power Network from High-Altitude Electromagnetic Pulse (HEMP)” July 13, 2009, Meta-R-314.

Appendix
E1 HEMP Myths

Much of the literature on HEMP is either classified or not easily accessible. Probably because of this, some of what is openly available tends to vary in accuracy – some, especially from the Internet, has major inaccuracies. Some discussions of HEMP have the right words and concepts, but do not quite have them put together right, or have inaccurate interpretations. Here we will discuss some common misunderstandings. HEMP has also appeared in some movies, and there are on-line discussions about possible errors in their depiction of HEMP. Here we will be concerned with E1 HEMP, and ignore misunderstandings about other types of EMP.

Extremists: Some general emphasis of comments fall into either "the world as we know it will come to an end" if there is a high altitude nuclear burst, or the other extreme: "it's not a big deal, nothing much will happen". Since we really have never had a nuclear burst over anything like our current modern infrastructure, no one really knows for sure what would happen, but both extremes are not very believable.

Yield: There appears to be an assumption that yield is important – it is not for E1. The assumption that E1 is an issue only for cold war type situations, but not for terrorists or rogue nations, is false. Very big bombs might have better area coverage of high fields by going to higher burst heights, but for peak fields the burst yield is only a very minor consideration.

1962 experience: Some point to the Starfish event, and the rather minor HEMP effects produced at Hawaii by it. However, there are many problems with extrapolating that experience:

1. That was about half a century ago. Since then the use of electronics has increased greatly, and the type of sensitive electronics we currently use did not really exist back then.
2. The burst was fairly far away from Hawaii, and the incident E1 HEMP was much less than worse case.
3. The island is small – if over the continental U.S., long transmission lines would be exposed (especially an issue for late-time HEMP). In addition, widely separated substations would have been exposed, although with electromechanical relays (not solid state).

Also the yield argument has been used – Starfish was a very big weapon, yet it did very little – see the previous item, yield is not really very significant.

Cars dying: Some say that all vehicles traveling will come to a halt, with all modern vehicles damaged because of their use of modern electronics (and one movie even had a bulk, non-electronic part dying). Most likely there will be some vehicles affected, but probably just a small fraction of them (although this could create traffic jams in large cities). A car does not have very long cabling to act as antennas, and there is some protection from metallic construction. As non-metallic materials are used more and more

in the future to decrease weight and increase fuel efficiency, this advantage may disappear.

Wristwatch dying: One movie critic pointed out that electronics in a helicopter were affected, but not the star's electronic watch. A watch is much too small for HEMP to affect it.

Electrons present: One critic, with some awareness of the generation process, said that HEMP could not be present unless there were also energetic electrons present. This is true when one is within the source region, which exists for all types of EMP – there are energetic electrons present. However for the HEMP, the radiation and energetic electrons are present at altitudes of 20 to 40 km, not at the ground.

Turn equipment off: There is truth to this recommendation (if there were a way to know that a burst was about to happen). Equipment is more vulnerable if it is operating, because some failure modes involving E1 HEMP trigger the system's energy to damage itself. However, damage can also happen, but not as easily, to systems that are turned off.

Maximum conductor length: There is a suggestion that equipment will be OK if all connected conductors are less than a specific length. Certainly shorter lengths are generally better, but there is no magic length value, with shorter always being better and longer not. Coupling is much too complex for such a blanket statement – instead it should be "the shorter the better, in general". (There can be exceptions, such as resonance effects, which depend on line lengths.)

Stay away from metal: There is a recommendation to be some distance away from any metal when a HEMP event occurs (assuming there was warning), because very high voltages could be generated. Metal can collect E1 HEMP energy, and easily generate high voltages. However, the "skin effect" (a term not really derived from the skin of humans or any other animal) means that if a human were touching a large "antenna" during an E1 HEMP event, any current flow would not penetrate into the body. Generally E1 HEMP is considered harmless for human bodies.